Published in final edited form as:
PET Clin. 2009 January ; 4(1): 101–128. doi:10.1016/j.cpet.2009.05.006.

Fluorine-18 Radiolabeled PET Tracers for Imaging Monoamine Transporters: Dopamine, Serotonin, and Norepinephrine

Jeffrey S. Stehouwer, PhD and **Mark M. Goodman, PhD***
Department of Radiology, Center for Systems Imaging, Emory University School of Medicine, Atlanta, GA, U.S.A.

Synopsis

This review focuses on the development of fluorine-18 radiolabeled PET tracers for imaging the dopamine transporter (DAT), serotonin transporter (SERT), and norepinephrine transporter (NET). All successful DAT PET tracers reported to date are members of the 3β-phenyl tropane class and are synthesized from cocaine. Currently available carbon-11 SERT PET tracers come from both the diphenylsulfide and 3β-phenyl nortropane class, but so far only the nortropanes have found success with fluorine-18 derivatives. NET imaging has so far employed carbon-11 and fluorine-18 derivatives of reboxetine but due to defluorination of the fluorine-18 derivatives further research is still necessary.

Keywords

Fluorine-18 PET; Tropanes; Dopamine Transporter; Serotonin Transporter; Norepinephrine Transporter

Introduction

The dopamine transporter (DAT), serotonin transporter (SERT), and norepinephrine transporter (NET) are plasma membrane biogenic monoamine transporters which belong to the family of Na^+/Cl^- dependent transporters.[1–8] In the central nervous system (CNS) the DAT, SERT, and NET are located on presynaptic neurons and function to remove their respective neurotransmitter from the synapse thereby terminating the action of that neurotransmitter. These three transporters have each been implicated in numerous psychiatric disorders such as depression, suicide, schizophrenia, Parkinson's Disease (PD), and attention-deficit hyperactivity disorder (ADHD) and are also the target of drugs of abuse such as cocaine, amphetamines, and MDMA (Ecstasy). As such, these transporters have become therapeutic targets to treat psychiatric disorders and drug addiction.[9–11] The ability to image the DAT, SERT, and NET with positron emission tomography (PET) or single-photon emission computed tomography (SPECT) may aid in the diagnosis and management of psychiatric disease by providing a means to measure the density of these transporters in specific brain

*Corresponding author: Mark M. Goodman, PhD, Wesley Woods Health Center, 2nd Floor, WWHC #208, Department of Radiology, 1841 Clifton, Road NE, Atlanta, GA 30329. Phone: (404) 727-9366. Fax: (404) 712-5689. mgoodma@emory.edu, Jeffrey S. Stehouwer, PhD, Wesley Woods Health Center, 2nd Floor, WWHC #209, Department of Radiology, 1841 Clifton, Road NE, Atlanta, GA 30329, Phone: (404) 712-1201. Fax: (404) 712-5689. jstehou@emory.edu.

regions.[12–17] Additionally, the availability of radiolabeled tracers for these transporters may aid in the development of new therapeutics by enabling the occupancy of the therapeutic to be measured.[18–24]

Numerous PET tracers for the DAT, SERT, and NET have been developed that are radiolabeled with carbon-11 but these are limited to use in the location where they are prepared and only allow for imaging times of up to about 2 hours due to the short half-life of ^{11}C ($t_{1/2}$ = 20.4 min).[25–27] The longer half-life of ^{18}F ($t_{1/2}$ = 109.8 min) allows for longer synthesis times and imaging sessions as well as for the transport of the ^{18}F-labeled tracer to locations away from the cyclotron facility which allows for PET imaging centers without onsite cyclotrons to employ these tracers. In addition to the longer half-life of ^{18}F, the positrons emitted from ^{18}F-nuclides have a lower maximum energy (0.64 MeV)[26] than the positrons emitted from ^{11}C-nuclides (0.97 MeV) which therefore deposits less energy into tissue and also results in a shorter linear range that allows for higher spatial resolution.[28,29] Radiolabeling tracers with ^{11}C is convenient due to the ubiquitous nature of carbon in organic compounds whereas fluorine is far less common. Fluorine, though, has been shown to impart unique properties to organic molecules and is now being exploited extensively in medicinal chemistry.[30–36] Thus, numerous methods have been developed to introduce ^{18}F or ^{19}F into molecules.[37–41] This review will focus on fluorine-18 radiolabeled PET tracers for imaging the DAT, SERT, and NET. Several carbon-11 PET tracers are also included to allow for comparisons in instances where a tracer can be radiolabeled with either isotope or where fluorinated analogs of existing ^{11}C-labeled tracers have been developed.

There are several performance criteria that should be met in order for a candidate brain PET tracer to become a useful tracer. High binding affinity to the target, especially if the target is of low density, will enable highly specific and selective binding to the target. The goal is to obtain the highest possible target-to-nontarget uptake ratios which will result in PET images with high signal-to-noise ratios. If the tracer does not bind strong enough to the target then the tracer will not be retained in the tissue of interest and will just pass through. But, if the tracer binds too strongly then it will not dissociate from the target during the course of the PET study and will accumulate in the tissue of interest and only blood flow will be measured. A balance must, therefore, be obtained which will allow for the achievement of peak uptake in the target tissue in a short time frame (^{18}F allows for longer time frames compared to ^{11}C) followed by a steady washout to allow for kinetic modeling of the behavior of the tracer.[42–47] Moderate lipophilicity in the range of log$P$ = ~1–3 is necessary to allow for rapid entry into the brain and to limit nonspecific binding. [48–50] Low binding to plasma proteins is necessary to make as many tracer molecules as possible available for brain entry. Metabolism of the tracer is unavoidable but the resulting metabolites that are generated in the periphery, if they are radiolabeled, should be hydrophilic so that they cannot enter the brain. The generation of radiolabeled metabolites in the brain is also undesirable and any radiolabeled metabolites that are produced should have little or no affinity for the target of interest. As will become apparent below, meeting all of these criteria simultaneously is a difficult task.

Dopamine Transporter (DAT)

The human DAT is a 620-amino acid transmembrane protein which is 98.9% homologous to the monkey DAT and 92% homologous to the rat DAT.[4,51–53] The DAT is found in high densities in the caudate, putamen, nucleus accumbens, and olfactory tubercle with lower densities in the substantia nigra, amygdala, and hypothalamus.[54–57] The DAT has been associated with numerous neuropsychiatric diseases including PD,[58–60] supranuclear palsy,[59] ADHD,[61] and Tourette's Syndrome.[62] The ability to image the DAT with PET may therefore aid in the diagnosis, monitoring, and treatment of these diseases.[13,15,17,63]

Early work towards developing an ^{18}F-labeled DAT imaging agent focused on the GBR-compounds[64,65] [^{18}F]**1** and [^{18}F]**2** (Figure 1).[66–71] PET imaging with [^{18}F]**2** in monkeys [72] showed rapid uptake into the striatum and cerebellum with maximum levels achieved within 2–3 min followed by a slow but steady washout. Washout was faster from the cerebellum than the striatum which resulted in a striatum-to-cerebellum ratio of 1.76 at the end of the study. Radiotracer uptake was highest in the liver and kidneys due to metabolism of the tracer but low bone uptake indicated that the aryl-fluorine bond was stable to metabolic defluorination. The imaging results with [^{18}F]**2** were promising but the tracer still suffered from high lipophilicity and non-specific binding. The synthesis and radiolabeling of the GBR-derivatives [^{18}F]**3** and [^{18}F]**4** has also been reported but imaging data was not included.[73]

Cocaine (**5**) (Fig 2, Table 1) binds to the DAT, SERT, and NET[74,75] but the DAT was initially implicated as the site related to substance abuse.[76–78] As a tool to study cocaine addiction [^{11}C]cocaine PET imaging has been employed[79–83] but imaging times are limited due to the short half-life of ^{11}C. 4′-[^{18}F]Fluorococaine ([^{18}F]**6**) allows for extended imaging studies due to the longer half-life of ^{18}F and [^{18}F]**6** was shown to have identical kinetic behavior to [^{11}C]cocaine in PET imaging studies.[82]

Cocaine metabolism can take several possible routes: (*a*) ester hydrolysis, (*b*) *N*-demethylation, (*c*) *N*-oxidation, (*d*) aryl hydroxylation and/or epoxidation, and (*e*) dehydrobenzoylation.[82, 84–89] The benzoic ester hydrolysis route was rendered obsolete when Clarke and co-workers demonstrated that replacement of the benzoyloxy group with a phenyl group attached directly to the 3β-position of the tropane skeleton produced compounds with higher binding affinities at the DAT than cocaine itself.[90] This new class of 3β-phenyl tropanes has been exploited extensively in the search for therapeutics to treat cocaine addiction[10,11,91–95] and hundreds of compounds have already been reported in the past[96] and more continue to be reported to this day.[97,98] The structures of some of the first 3β-phenyl tropane compounds prepared, **7**–**12**, are shown in Fig 2 and Table 1.[90–92,99] The high affinity of these compounds for the DAT naturally made them candidates for use as PET tracers when labeled with ^{11}C as they can all be labeled on either the *N*-methyl group or the methyl ester.[88,100–104] Unfortunately, these ^{11}C-labeled compounds do not reach binding equilibrium during the course of the imaging study which limits their usefulness in kinetic modeling. Furthermore, compound **11** has a similar affinity for the DAT and SERT and compounds **9** and **10** are only slightly selective for the DAT over the SERT[94,96,105] thus limiting the utility of these compounds as DAT-selective imaging agents.

Out of compounds **7**–**12**, only compound **8** contains a ^{19}F atom that could be replaced with ^{18}F. Additionally, **8** is more selective for the DAT over the SERT and NET than compounds **9**–**11**,[94,96] and previous work with [^{11}C]**8** had demonstrated that it was capable of imaging the DAT.[100,101] Thus, [^{18}F]**8** was synthesized and evaluated by biodistribution studies in rats[106] and then by PET imaging in humans.[107] In rat brain the striatum-to-cerebellum ratio reached a maximum of ~9.6 after 2 h and this uptake could be blocked by pretreatment with the DAT ligand GBR 12909 (**1**).[64,65] In rat biodistribution studies the highest uptake at all times was observed in the liver and urine whereas uptake in the kidney, spleen, and lungs was initially high but then decreased. Very little bone uptake was observed indicating that the aryl-fluorine bond of [^{18}F]**8** is stable to metabolic defluorination, similar to what was observed for [^{18}F]**2**. In human subjects the total activity of [^{18}F]**8** in the caudate and putamen peaked at 225 min and then slowly declined whereas the specific binding remained at a plateau from 3–5 h post-injection. Application of [^{18}F]**8** to studying human subjects with early PD demonstrated that [^{18}F]**8** was capable of detecting presynaptic dopaminergic hypofunction.[108]

In an effort to reduce the time required to reach peak uptake of [^{18}F]**8**, the *N*-[^{18}F]fluoroethyl [105] and *N*-[^{18}F]fluoropropyl[109,110] derivatives, [^{18}F]**13** and [^{18}F]**14**, respectively, were prepared. In vitro binding assays demonstrated that both **13** and **14** had a reduced affinity for the DAT, SERT, and NET relative to **8**, but **13** and **14** both had a slightly improved selectivity for the DAT over the SERT relative to **8**.[105] PET imaging with [^{18}F]**13** in conscious rhesus monkeys demonstrated that [^{18}F]**13** reaches peak uptake after about 20 min followed by a washout phase, thus demonstrating reversible binding. A comparison study with [^{11}C]**8** showed only irreversible binding during the 91 min PET scan as the radioactivity continuously increased throughout the study. Therefore, replacing the *N*-methyl group of **8** with an *N*-fluoroethyl group as in **13** resulted in improved tracer performance. A blocking study with **1** demonstrated that [^{18}F]**13** binding was DAT-specific. Metabolite analysis of [^{18}F]**13** in plasma showed only polar metabolites and no lipophilic metabolites that could cross the blood-brain barrier. Compound [^{18}F]**14** was evaluated ex vivo in rats and demonstrated rapid entry into the brain with a striatum-to-cerebellum ratio of ~3.1 after 5 min followed by a continuous decrease. This uptake could be blocked by pretreatment with **1**. A continuous uptake was observed in the skull indicating a slow defluorination of the [^{18}F]fluoropropyl group.

Compound **11** has a nearly equal affinity for the DAT and SERT[94,96,105] and PET imaging with [^{11}C]**11** showed uptake in the striatum as well as the thalamus and neocortex.[88,103] This uptake in the thalamus and neocortex could be displaced by the SERT ligand citalopram [111,112] thus demonstrating binding to both the DAT and SERT in vivo, which is in agreement with the in vitro binding data.[96,105,113] In an effort to obtain ^{18}F-labeled derivatives of **11** the *N*-fluoroalkyl compounds **15** and **16** were prepared.[113,114] Replacement of the *N*-methyl group of **11** with an *N*-fluoroethyl group (**15**) or an *N*-fluoropropyl group (**16**) resulted in a reduced binding affinity at the DAT and NET but an increased binding affinity at the SERT relative to **11**.[113] Replacement of the methyl ester group of **16** with an isopropyl ester to give **17** increased the binding affinity at the DAT relative to **11** and significantly reduced the binding affinity at both the SERT and NET.[113,115] A SPECT imaging comparison[116] of [^{123}I]**15**, [^{123}I]**16**, and [^{123}I]**17** in baboons demonstrated that [^{123}I]**15** and [^{123}I]**16** had higher peak uptake in the striatum than [^{123}I]**17** thus ruling out [^{123}I]**17** for adaptation to PET imaging as [^{18}F]**17**. Additionally, [^{123}I]**15** had more rapid kinetics than [^{123}I]**16**. Comparison between [^{123}I]**11** and [^{123}I]**16** in humans with SPECT imaging showed that [^{123}I]**16** had higher non-specific binding than [^{123}I]**11** but a lower radiation burden to the basal ganglia.[117]

PET studies in anesthetized cynomolgus monkeys with [^{11}C]**15** showed high uptake in the putamen with lesser uptake in the thalamus and neocortex.[118] A blocking study with **1** reduced the uptake of [^{11}C]**15** in the putamen by 75 % but did not affect the uptake in the thalamus or neocortex thus indicating that SERT binding was still an issue. Compound [^{18}F]**16** has been radiolabeled and evaluated in anesthetized cynomolgus monkeys[119] and conscious humans.[120] In monkeys high uptake of [^{18}F]**16** was observed in the putamen (this was blockable with **1**) with peak uptake achieved in 30–40 min followed by only a very slight washout. After 70 min the striatum-to-cerebellum ratio was 4.5–5. Uptake in the thalamus was at levels similar to the cerebellum thus demonstrating an improvement over [^{11}C]**11**, [^{11}C]**15**, and [^{11}C]**16**. Metabolite analysis did not detect any lipophilic metabolites but [^{18}F]fluoride was detected in plasma indicating that defluorination was occurring. Initial studies in humans with [^{18}F]**16** showed high uptake in the putamen of a healthy normal volunteer whereas uptake was reduced 65% in a PD patient.[120] Additional studies[121] in healthy normal humans with [^{18}F]**16** showed that uptake in the striatum increased rapidly after injection but then leveled off after 40 min and did not wash out. Uptake in the thalamus peaked at ~20 min and then began to wash out. In PD patients uptake in the putamen peaked at 30 min and then slowly washed out. Additional studies have been performed with [^{18}F]**16** to acquire data for parametric mapping,[122] dosimetry,[123] and modeling.[124] A one-step high-yield radiosynthesis of [^{18}F]**16** has been developed.[125]

Compounds **18** and **19** are the *N*-fluoroalkyl derivatives of **9** which has been previously radiolabeled as [^{11}C]**9** and evaluated in rats.[102] PET studies with [^{18}F]**19** in anesthetized rhesus monkeys showed high uptake in the striatum with putamen-to-cerebellum and caudate-to-cerebellum ratios of 3.35 and 2.28, respectively, after 115 min.[126] The uptake in the cerebellum washed out after an initial peak at 13.5 min but the uptake in the caudate and putamen remained nearly constant after peaking thus indicating irreversible binding to the DAT. Biodistribution studies in rats showed continuously increasing bone uptake indicating that the fluoropropyl group was not resistant to defluorination which is in agreement with the detection of [^{18}F]fluoride in plasma reported for the metabolism of [^{18}F]**16** and the observed skull uptake in studies with [^{18}F]**14**. PET imaging with [^{18}F]**18** in an anesthetized rhesus monkey showed high uptake in the caudate and putamen (displaceable with **11**) with peak uptake achieved in 60–75 min followed by washout at a rate of 8%/h.[127] At 115 min the putamen-to-cerebellum ratio was 12.7 and the caudate-to-cerebellum ratio was 12.3. When an imaging study with [^{18}F]**19** was performed in the same rhesus monkey the uptake in the caudate and putamen continuously increased throughout the course of the study,[127] similar to what was previously reported.[126] Thus, [^{18}F]**18** displays reversible binding and can achieve binding equilibrium whereas [^{18}F]**19** binds irreversibly. Compound [^{18}F]**18** has since been used to measure DAT occupancy of cocaine[128] and radiation dosimetry studies have been performed in rats and monkeys.[129,130] Two different automated radiosynthesis methods of [^{18}F]**18** have been reported.[131,132] Initial studies[133] in 6 healthy humans with [^{18}F]**18** showed that the time for peak uptake in the caudate and putamen was in the range of 70–130 min with caudate-to-cerebellum ratios of 7.6–10.5 and putamen-to-cerebellum ratios of 7.1–9.3. Comparison of the data obtained in healthy humans to that obtained in PD patients demonstrated that [^{18}F]**18** has the potential to measure DAT density in the brain and to detect the reduction in DAT density that is associated with PD. Metabolism studies in humans using arterial samples after injection of [^{18}F]**18** identified a polar non-ether-extractable component.[133] Subsequent studies[134] in rats, monkeys, and humans identified this polar metabolite as either [^{18}F]fluoroethanol, [^{18}F]fluoroacetaldehyde, or [^{18}F]fluoroacetic acid (or a combination of all three as they are metabolically interchangeable). This work demonstrated that the polar metabolite is generated in the periphery but then passes into the brain and distributes evenly throughout the brain. The authors therefore suggest that the tissue reference method should not be used for analyzing PET data obtained with [^{18}F]**18** but rather an arterial input function should be used.

This *N*-dealkylation of [^{18}F]**18** is not unique to [^{18}F]**18** but has also been observed with cocaine,[84] [^{11}C]cocaine (to give [^{11}C]CO_2 in baboons),[79,82] and [^{11}C]**11**,[88] as well as other tracers.[135–139] Thus, metabolic cleavage of radiolabeled *N*-methyl and *N*-fluoroethyl groups is unavoidable and it should be expected that any tracer radiolabeled with an *N*-[^{18}F]fluoroethyl group will be metabolized in the periphery to [^{18}F]fluoroethanol, [^{18}F]fluoroacetaldehyde, or [^{18}F]fluoroacetic acid, and such an effect has recently been reported with the amyloid imaging agent [^{18}F]FDDNP.[140] Switching to an *N*-[^{18}F]fluoropropyl group is not necessarily a better alternative because the *N*-[^{18}F]fluoropropyl group is not stable to defluorination as was demonstrated with [^{18}F]**14**, [^{18}F]**16**, and [^{18}F]**19**.

Compounds **20** and **21** are the *N*-fluoropropyl derivatives of **12** and **10**, respectively. A procedure for preparing [^{18}F]**20** has been reported but imaging data was not included.[141] PET imaging with [^{18}F]**21** in baboons showed the highest uptake in the putamen with peak uptake achieved in 7–10 min. The washout half-life was 54 min for the striatum whereas it was 19 min for the midbrain and 16 min for the cerebellum. A striatum-to-cerebellum ratio of 3.3 was achieved at 45–60 min post injection. Metabolite analysis detected a “less-lipophilic” metabolite which was presumed to be the 2β-carboxylic acid resulting from hydrolysis of the methyl ester.

As an alternative to radiolabeling with *N*-fluoroalkyl groups several compounds containing fluoroethyl esters have been prepared (**22**–**25**). Biodistribution studies in rats with [^{18}F]**22** and [^{18}F]**23** showed high uptake in the striatum and olfactory tubercles.[102] Compound [^{18}F]**23** showed higher uptake in the striatum than [^{18}F]**22** but also significantly higher liver uptake. Bone uptake was minimal for both tracers indicating that the [^{18}F]fluoroethyl ester was stable to defluorination. An improved synthesis and metabolic stability analysis in rats of [^{18}F]**23** has recently been reported.[142] This work found that after 3 h plasma radioactivity consisted of ~93% intact [^{18}F]**23** and the radioactivity in homogenized cerebrum and cerebellum extracts each consisted of ~96% intact [^{18}F]**23**. Furthermore, there was no trace of [^{18}F] fluoroacetaldehyde or [^{18}F]fluoroacetic acid which would result from hydrolysis of the [^{18}F] fluoroethyl ester.

Compounds **24** and **25** are the fluoroethyl ester derivatives of **10** and **11**, respectively.[143, 144] Biodistribution studies of [^{18}F]**24** in rats showed high uptake in the striatum (blockable with **1**) with peak uptake around 60 min followed by a slow washout.[145] Uptake in the adrenals and kidneys was initially high but then washed out whereas uptake in the liver continuously increased throughout the study. The tracer was rapidly metabolized in rat plasma to a polar metabolite which accounted for 85% of radioactivity in plasma after 60 min. In rat striatal homogenates the radioactivity was >90% intact parent compound after 60 min. Low bone uptake in the biodistribution studies indicated that the [^{18}F]fluoroethyl ester was stable to defluorination. The striatal uptake observed in the biodistribution studies was further confirmed by autoradiography. MicroPET studies with [^{18}F]**24** in rats showed a steady uptake in the striatum for the first 20 min which then peaked and remained stable for 30–100 min post-injection. At the end of the study (115 min p.i.) the striatum-to-cerebellum ratio was 2.8. Evaluation of [^{18}F]**25** in rats showed peak uptake in the striatum at 15 min followed by a steady washout.[146] At 60 min the striatum-to-cerebellum ratio was 3.73 and the striatum-to-thalamus ratio was 2.99, while at 120 min the thalamus-to-cerebellum ratio was 1.65. High uptake in the kidneys suggested a renal excretion route whereas low bone uptake indicated stability to defluorination. A metabolic stability study with porcine carboxyl esterase found that [^{18}F]**25** and [^{123}I]**11** have similar stabilities in regards to resistance to enzymatic hydrolysis of the ester but this stability was less than that found for [^{123}I]**16**.[147] The authors suggest that the *N*-fluoropropyl group of [^{123}I]**16** is bulky enough to impede access to the ester bond by the enzyme thus inhibiting this route of metabolism. This bulkiness of the *N*-[^{18}F] fluoropropyl group and the subsequent prevention of ester hydrolysis may, therefore, account for why defluorination of [^{18}F]**14**, [^{18}F]**16**, and [^{18}F]**19** is observed as the major metabolic route.

It had been previously shown that replacing the methyl ester of **9** with an isopropyl ester significantly reduced binding affinity at the SERT and NET while only slightly reducing DAT binding affinity.[115] Thus, the fluoroisopropyl derivatives (*R*)-**26** and (*S*)-**26** (Figure 3) were prepared and evaluated.[148] Competitive binding assays in murine kidney cells with transfected DAT or SERT showed that (*S*)-**26** had a nearly 5-fold higher affinity (K_i = 0.67 nM) than (*R*)-**26** (K_i = 3.2 nM) at the DAT and a lower affinity at the SERT (K_i's = 85 nM (*S*) and 65 nM (*R*)). For comparison, **11** was included and had binding affinities of K_i = 0.48 nM (DAT) and K_i = 0.67 nM (SERT) which is in agreement with the previously reported nearly equal affinities at each transporter.[96,105,113] Thus, (*S*)-**26** has only a slight reduction in DAT affinity compared to **11** but has a significant improvement in DAT vs. SERT selectivity. Biodistribution studies in rats with [^{18}F](*R*/*S*)-**26** showed highest uptake in the liver but very little bone uptake indicating that the fluoroisopropyl ester was stable to defluorination. In rat brain biodistribution studies [^{18}F](*R*)-**26** reached peak uptake in the striatum at 30 min and had a striatum-to-cerebellum ratio of 6.0 at 60 min, whereas [^{18}F](*S*)-**26** also reached peak uptake in the striatum at 30 min but at 60 min the striatum-to-cerebellum ratio was 11.8 and at 120 min it was 12.7. This higher uptake ratio for [^{18}F](*S*)-**26** compared to [^{18}F](*R*)-**26** is in

agreement with the higher in vitro DAT binding affinity observed for [^{18}F](*S*)-**26**. PET imaging in rhesus monkeys with [^{18}F](*R*)-**26** and [^{18}F](*S*)-**26** showed that for [^{18}F](*R*)-**26** uptake peaked in the putamen and caudate around 45 min and remained nearly stable until the end of the study (115 min) while uptake of [^{18}F](*S*)-**26** was still increasing at 115 min when the study ended. At 115 min [^{18}F](*R*)-**26** had a putamen-to-cerebellum ratio of 3.5 and a caudate-to-cerebellum ratio of 2.5 whereas [^{18}F](*S*)-**26** had a putamen-to-cerebellum ratio of 2.5 and a caudate-to-cerebellum ratio of 2.5. Additionally, the cerebellum uptake washed out significantly faster for [^{18}F](*R*)-**26** than for [^{18}F](*S*)-**26** which allowed [^{18}F](*R*)-**26** to achieve a transient equilibrium at 75 min. Metabolite analysis of rhesus monkey arterial plasma indicated that both [^{18}F](*R*)-**26** and [^{18}F](*S*)-**26** are metabolized to a non-ether-extractable polar compound but that [^{18}F](*R*)-**26** is metabolized more rapidly with 25% unmetabolized [^{18}F](*R*)-**26** remaining after 14 min but 30% unmetabolized [^{18}F](*S*)-**26** remaining after 30 min.

Other variations on the tropane structure have included the *N*-benzyl 2β-ethyl ketones **27** and **28**.[149] PET studies in rhesus monkeys with [^{18}F]**27** and [^{18}F]**28** demonstrated that both tracers reached peak uptake in the basal ganglia in ~20 min followed by a steady washout, thus indicating reversible binding. Compound [^{18}F]**28** was the superior of the two tracers with a basal ganglia-to-cerebellum uptake ratio of 2.6 vs. 1.5 for [^{18}F]**27**, presumably due to the higher affinity [^{18}F]**28** has for the DAT.[149] Both tracers were rapidly metabolized in a rhesus monkey with <30% [^{18}F]**27** remaining and <20% [^{18}F]**28** remaining after 20 min. Metabolite analysis of arterial plasma samples from both a rhesus monkey and rats showed that [^{18}F]**28** was metabolized to a lipophilic metabolite but this metabolite was not observed in rat whole brain samples indicating that the metabolite cannot cross the blood-brain barrier.

The *N*-(*E*)-fluorobutenyl tropanes **29**–**32** (Fig 4, Table 2) have been previously reported.[150,151] Subsequently, the tolyl-derivative **33** was also reported.[152–156] Compounds **29**–**33** are thus the *N*-(*E*)-fluorobutenyl derivatives of **8**–**12**, respectively. The binding affinities of **29**–**32** are shown in Fig 4 and Table 2.[151] Compounds **31** and **32** have a high affinity at both the DAT and SERT with little or no selectivity, similar to what has been reported for **10** and **11**.[11,96,105,113,148] Compound **30** has a reduced affinity at the DAT and SERT relative to **31** and **32** without a significant improvement in selectivity. Compound **29** has a 10-fold lower affinity at the DAT than **32** along with a greatly reduced affinity at the SERT which results in a significantly improved selectivity for the DAT over the SERT compared to **30**–**32**.

Our initial imaging work with [^{18}F]**30**-[^{18}F]**32** was performed on a Siemens 951 PET scanner. We have since reevaluated [^{18}F]**30** and [^{18}F]**31** along with [^{18}F]**29** in anesthetized cynomolgus monkeys with a Concorde microPET P4 which allows for higher resolution images.[157] The highest uptake of [^{18}F]**29** is seen in the putamen with peak uptake achieved after 25 min followed by a steady washout. Uptake in the caudate is also high but less than that seen in the putamen. This uptake in the caudate peaks after ~30 min but then remains stable until ~100 min post-injection followed by only a slight washout. Uptake in the substantia nigra peaks after 10 min and then slowly washes out, whereas uptake in the cerebellum peaks after 10 min and rapidly washes out. Injection of the DAT ligand RTI-113[158–161] at 90 min post-injection completely displaces [^{18}F]**29** from the caudate and the putamen. Compound [^{18}F]**30** shows a rapid uptake in the putamen with peak uptake achieved after 20 min followed by only a slight washout. Uptake in the caudate increases rapidly for the first 20 min, then increases slowly for 20–90 min, and then remains level for 90–235 min. The uptake in the caudate is less than that observed in the putamen and remains less than in the putamen even after the slight washout of activity from the putamen. The uptake in the substantia nigra peaks after 15 min and then washes out at a slower rate than that observed for [^{18}F]**29**. Uptake of [^{18}F]**31** in the putamen peaks after 30 min and only slightly washes out whereas uptake in the caudate peaks after 30 min and then remains constant for 30–235 min. The initial uptake in the putamen was 1.5x that observed in the caudate. Uptake in the substantia nigra peaked after 20 min and then washed

out steadily but slower than that observed for [^{18}F]**29**. This rapid and high uptake of [^{18}F]**30** and [^{18}F]**31** in the putamen and the caudate followed by a lack of washout is similar to that reported for [^{11}C]**33**.[152,153,156]

Compounds [^{18}F]**29**-[^{18}F]**31** and [^{11}C]**33** all show higher uptake in the putamen than in the caudate. It has been previously shown that anesthesia can influence the behavior of PET tracers and can cause trafficking of the DAT to the plasma membrane.[162–168] Therefore, in an effort to evaluate whether the uptake observed for [^{18}F]**29**-[^{18}F]**31** was influenced by the anesthesia used in the microPET studies a PET study with [^{18}F]**29** was performed in an awake rhesus monkey on a Siemens/CTI high resolution research tomograph (HRRT).[157] The uptake of [^{18}F]**29** in the caudate and putamen was equal in each hemisphere of the brain in the awake rhesus monkey thus indicating that the higher uptake in the putamen relative to the caudate observed in the microPET studies with [^{18}F]**29**-[^{18}F]**31** was most likely an anesthesia effect. This is presumably also the cause of the higher uptake observed in the putamen than in the caudate with [^{11}C]**33** in an anesthetized baboon as well as the reported putamen-to-cerebellum and caudate-to-cerebellum uptake ratios of 30 and 24.6, respectively, in one study [152] and 28.9 and 23.6, respectively, in another study.[153] The uptake of [^{18}F]**29** in the putamen and the caudate of the awake rhesus monkey peaked at 30 min and then slowly washed out until the end of the study (85 min), whereas the uptake ratios peaked around 60 min and then began to decline. Thus, [^{18}F]**29** is able to achieve peak uptake, reversible binding, and attain a transient equilibrium in an acceptable time frame while also achieving excellent uptake ratios vs. cerebellum uptake in an awake state.

The microPET images obtained with [^{18}F]**29**-[^{18}F]**31** and the PET images obtained with [^{18}F]**29** all show skull uptake thus indicating defluorination of the [^{18}F]-(*E*)-fluorobutenyl group. In an effort to by-pass this [^{18}F]-defluorination and eliminate bone uptake of [^{18}F]fluoride we are currently working towards radiolabeling [^{18}F]**29** on the aromatic ring similar to what has been reported for [^{18}F]**1**-[^{18}F]**4**, [^{18}F]**6**, and [^{18}F]**8**. Skull uptake of [^{18}F]fluoride resulting from defluorination of [^{18}F]**33** can be avoided by using [^{11}C]**33** but both [^{18}F]**33** and [^{11}C]**33** presumably will still suffer from benzylic hydroxylation and the generation of radiolabeled metabolites similar to what has recently been reported for [^{11}C]PE2I.[139,147] It is expected that the size of the *N*-(*E*)-fluorobutenyl group will prevent enzymatic hydrolysis of the methyl ester similar to what has been previously reported.[147]

Extensive research over the past 20 years directed at developing fluorine-18 radiolabeled PET tracers for imaging the DAT has identified numerous potential candidates from the 3β-phenyltropane class. The most promising are those that can achieve reversible binding and a transient equilibrium in a short time frame along with high specific binding and selectivity while also minimizing the interference from radiolabeled metabolites. So far both [^{18}F]**16** and [^{18}F]**18** have found use in human imaging and both have demonstrated their utility in detecting a reduction of DAT density in human PD subjects. But both compounds show a slower washout than may be desirable and both suffer from complications due to metabolism. Compound [^{18}F]**29** offers improved kinetics but it will need to be radiolabeled on the aromatic ring in order to avoid the skull uptake that results from defluorination of the [^{18}F]fluorobutenyl group.

Serotonin Transporter (SERT)

The human SERT is a 630-amino acid protein[6] that is 98.6% homologous to rhesus monkey SERT, 93% homologous to mouse SERT, and 90% homologous to rat SERT.[4,169] The SERT is found in high densities in the dorsal and median raphe nuclei, putamen, caudate, thalamus, hypothalamus, and amygdala, with lower levels in the cortex and still lower levels in the cerebellar cortex.[170–177] The serotonin system has been associated with numerous psychiatric conditions including PD,[178,179] obsessive-compulsive and panic disorders,

[180] stress,[181] and depression and suicide.[182–184] A reduced density of SERT has been observed postmortem in depressed individuals and victims of suicide.[185–187] The SERT is, therefore, the target of the selective serotonin reuptake inhibitor (SSRI) class of antidepressants.[111,112] The availability of specific and selective SERT PET tracers would allow for the measurement of SERT density in the brain and may allow for the detection and diagnosis of SERT-related psychiatric illness as well as a means of measuring SSRI occupancy and the monitoring of SSRI therapy.[16,188–192]

The SSRI Fluoxetine (Prozac) **34**[193] (Figure 5) has been radiolabeled with both ^{11}C[194] and ^{18}F.[195] In both cases the uptake of the tracer was characterized by non-specific binding and high lipophilicity. A PET study with [^{18}F]**34** in rhesus monkeys showed uptake in all brain regions and an autoradiographic study in rats demonstrated irreversible binding due to subcellular uptake of the tracer.

The antidepressant (+)-McN5652[196] **35** has been radiolabeled with ^{11}C and evaluated in rats and mice[197] and in humans.[198] In the human brain the uptake of [^{11}C]**35** in the midbrain reached a plateau after ~90 min but did not wash out before the end of the study (115 min) thus necessitating the need for the longer-lived ^{18}F. The fluorinated derivatives **36** and **37** were therefore prepared and evaluated. Ex vivo autoradiography with [^{18}F]**37** in mice showed accumulation in the hypothalamus, substantia nigra, and raphe nuclei but whole-brain uptake, specific binding, and tissue-to-cerebellum ratios were significantly less than that observed for [^{11}C]**35**. Replacement of the methyl group of **35** with a fluoromethyl group to give **36** resulted in about a 3-fold loss in binding affinity at the SERT.[199] Biodistribution studies in rats with [^{18}F]**36** showed uptake in the raphe nuclei, substantia nigra, locus coeruleus, hypothalamus, thalamus, and amygdala, and this uptake could be blocked with **34**.[200] The uptake in these regions washed out slower than cerebellum washout and this resulted in uptake ratios of 7–9 after 3 h. High uptake was also observed in the adrenal gland, lung, intestine, spleen, kidney, liver, and bone marrow. A continuous increase of radioactivity in the skull indicated that [^{18}F]**36** was not stable to defluorination in rats. Additional studies with [^{18}F]**36** were performed in pigs.[201–203]

The fluorinated derivatives of 6-nitroquipazine,[204] **38** and **39**, have been prepared and evaluated as possible SERT PET tracers.[205,206] In rats [^{18}F]**38** rapidly entered the brain and showed the highest accumulation in the frontal- and posterial cortex followed by the striatum and this uptake could be reduced 10–20% with the SSRI citalopram.[111,112] Lesser uptake was observed in the thalamus but this uptake could be reduced 20–30% with citalopram. PET imaging in a monkey showed rapid uptake into the brain with a frontal cortex-to-cerebellum ratio of 1.53 and a striatum-to-cerebellum ratio of 1.25 at 80 min post-injection. The uptake in the thalamus was less than that observed in the cerebellum indicating that [^{18}F]**38** was not a good candidate for imaging the SERT. Biodistribution studies in mice with [^{18}F]**39** showed the highest uptake after 60 min in the frontal cortex and the lowest uptake in the cerebellum. High uptake was also observed in the olfactory tubercle, hypothalamus, thalamus, hippocampus, and striatum. Continuous bone uptake was also observed indicating a slow defluorination of the fluoropropyl group.

The diphenylsulfide **40** (Figure 6, Table 3) has been previously reported to be an inhibitor of the SERT and NET.[207,208] Numerous compounds have now been reported which exploit the diphenylsulfide motif in order to take advantage of its high binding affinity at the SERT and compounds **41**–**51** have been radiolabeled with ^{11}C.[209–218] Comparison of [^{11}C]**35**, [^{11}C]**41**, [^{11}C]**42**, [^{11}C]**44**, and [^{11}C]**49** indicated that [^{11}C]**42** had the fastest kinetics whereas [^{11}C]**49** had the highest signal-to-noise ratio.[213] Comparison between [^{11}C]**42** and [^{11}C]**45** in the same anesthetized rhesus monkey indicated that [^{11}C]**45** achieved higher uptake ratios than [^{11}C]**42** and also reached peak uptake faster.[218] Both [^{11}C]**42** and [^{11}C]**45** have been

employed in humans[219–221] and both have demonstrated that they are valuable tracers for imaging the SERT with PET, but both are ^{11}C-labeled and are still, therefore, limited to use where they are prepared and to imaging sessions of less than 2 h.

Compounds **47**, **49**, and **50** all have a high affinity for the SERT and are selective for the SERT over the DAT and NET. Compound **51** has a slightly reduced SERT affinity but still shows selectivity over the DAT and NET.[223] Compounds [^{11}C]**47**, [^{11}C]**49**, and [^{11}C]**50**, have been evaluated in baboons.[214–216] Biodistribution studies in rats were performed to compare [^{18}F]**47**, [^{18}F]**49**, [^{18}F]**50**, and [^{18}F]**51**.[223] All four compounds rapidly entered the brain and accumulated in the thalamus, hypothalamus, frontal cortex, striatum, and hippocampus. This uptake could be blocked with citalopram thus demonstrating SERT-specific binding. Compound [^{18}F]**49** reached peak uptake after 30 min followed by washout and this uptake was the highest among the four tracers. Compounds [^{18}F]**47**, [^{18}F]**50**, and [^{18}F]**51** all reached peak uptake after 10 min followed by washout while the highest uptake observed was with [^{18}F]**47**. PET imaging comparisons in the same baboon with [^{18}F]**47**, [^{18}F]**49**, and [^{18}F]**50** showed that [^{18}F]**47** and [^{18}F]**50** reached peak uptake in the thalamus in 15–35 min whereas [^{18}F]**49** reached peak uptake in 40–60 min but showed significantly higher specific binding.[228] Another reported biodistribution study in rats with [^{18}F]**47** had shown peak uptake at 30 min followed by washout.[222] This study also showed that [^{18}F]**47** accumulated rapidly in the muscle, lung, liver, and kidney but then cleared whereas bone uptake continuously increased indicating that, at least in rats, defluorination was a problem. In a PET study with [^{18}F]**47** in a baboon the radioactivity in the skull did not increase with time suggesting that defluorination was isolated to rats.[222] In this PET study peak uptake in the midbrain and striatum was reached in ~30–40 min with midbrain-to-cerebellum ratios of 3.2 at 2 h and 4.2 at 3 h and striatum-to-cerebellum ratios of 2.4 at 2 h and 2.7 at 3 h.

Compound **52** is an isomer of **47** where the fluorine atom has been moved from the 4-position (*para* to the sulfur atom) to the 5-position (*meta* to the sulfur atom). This change resulted in a significant loss in affinity for the SERT[224] compared to **47**[222] as well as a slight decrease in lipophilicity (log*P* = 2.47 vs. 2.73). Biodistribution studies in rats with [^{18}F]**52** showed an initial high uptake in the lungs, kidneys, and heart but this cleared quickly whereas bone uptake continued to increase indicating defluorination.[229] Brain uptake was rapid with peak uptake at 2 min followed by a fast washout. The hypothalamus-to-cerebellum ratio was 2.97 at 60 min which is less than that observed with [^{18}F]**47**. Thus, changing the position of the fluorine-atom did not produce an improvement in imaging properties compared to [^{18}F]**47**.

Compound **53** retains the fluorine atom in the 5-position and places a chlorine atom in the 4-position which produced a compound with a high SERT affinity and selectivity.[225] Biodistribution studies with [^{18}F]**53** in rats showed initial high accumulation in lung, muscle, liver, kidney, and skin which then declined.[225] Bone uptake was slightly less than that observed with [^{18}F]**52**[229] and significantly less than that observed with [^{18}F]**47**.[222] Brain uptake of [^{18}F]**53** was rapid with the highest uptake observed at 2 min followed by washout. At 60 min the hypothalamus-to-cerebellum ratio was 3.5 (compared to 3 for [^{18}F]**52**) and the striatum-to-cerebellum ratio was 2.9. Thus, [^{18}F]**52** and [^{18}F]**53** behave similarly in rats with regards to uptake ratios and defluorination but both have too rapid of kinetics when compared to [^{18}F]**47**.

The fluoroalkyl ethers **54**–**60** have a high affinity for the SERT but **54** and **58** also have an appreciable affinity for the NET [226] which may cause interference in PET imaging if the cerebellum was to be used as the reference region. In rat biodistribution studies [^{18}F]**55**-[^{18}F]**57**, [^{18}F]**59**, and [^{18}F]**60** showed high brain uptake but slow washout whereas [^{18}F]**54** and [^{18}F]**58** also showed high brain uptake but a faster washout. Of compounds [^{18}F]**54**-[^{18}F]**60**, the highest hypothalamus-to-cerebellum ratios were observed with [^{18}F]**54** and [^{18}F]**58** (~7.8

and ~7.7, respectively, at 120 min) due to the faster washout of these compounds.[226] Additional rat biodistribution studies with [^{18}F]**58** showed initial high uptake in the lung, skin, muscle, liver, and kidney which then slowly declined.[230] Bone uptake was high and remained high indicating defluorination. Brain uptake was rapid followed by a steady washout. Autoradiography showed uptake in the olfactory tubercles, thalamic nuclei, hypothalamic nuclei, substantia nigra, superior colliculus, dorsal raphe, medial raphe, and locus coeruleus, all of which could be blocked with the SSRI escitalopram[231,232] except for the locus coeruleus which could be blocked with the NET ligand nisoxetine.[233,234] Thus, some NET binding in the locus coeruleus is observed in conjunction with the desired binding in the SERT-rich brain regions when performing autoradiography but uptake in the cerebellum was not observed in the rat when PET imaging was performed with [^{18}F]**58** which will, therefore, allow for use of the cerebellum as the reference region. In the rat PET images obtained with [^{18}F]**58**, clear localization was observed in the thalamus, midbrain, and striatum with peak uptake achieved in 10–20 min followed by a steady washout.[230] The region-to-cerebellum ratios peaked at 100–110 min with a value of ~4 followed by a slow decline. The uptake in the midbrain, thalamus, and striatum could be displaced by escitalopram (2 mg/kg) but also, to a lesser extent, by nisoxetine (10 mg/kg). A similar displacement of the SERT PET tracer [^{11}C]*m*ZIENT during a chase study with the NET ligand (±)-reboxetine•mesylate (1 mg/kg) has also been observed.[235] Both nisoxetine and reboxetine[236] have a weak affinity for the SERT (K_i = 30 and 60 nM, respectively) but are selective for the NET over the SERT (21.4 and 6.7, respectively).[237] This weak binding to the SERT may be the cause of the observed displacement of these two tracers but alternatively, the displacement may be an indirect effect mediated through interactions between the noradrenergic and serotonergic systems.[238–240]

Compound **61** is a fluorinated derivative of **45**.[227] Introduction of the fluorine atom resulted in a slight reduction in SERT affinity but also a reduction in DAT and NET affinity which produced similar selectivities for the SERT over the DAT and NET. The presence of the fluorine atom also increased the lipophilicity somewhat (log$P_{7.4}$ = 2.06 and 1.60, respectively). MicroPET imaging with [^{11}C]**61** in an anesthetized cynomolgus monkey showed high uptake in the midbrain, pons, thalamus, and medulla with little uptake in the frontal cortex and cerebellum. No uptake was observed in the caudate or putamen which is surprising since this brain region does contain SERT.[177] Peak uptake of [^{11}C]**61** in the midbrain occurred between 12.5 and 27.5 min post-injection followed by a steady washout. At 85 min the midbrain-to-cerebellum ratio was 3.4 and the thalamus-to-cerebellum ratio was 2.3. The observed uptake was displaceable with (*R*/*S*)-citalopram•HBr thus demonstrating SERT-selective binding. These promising results suggest that [^{18}F]**61** may be a viable SERT PET tracer.

Replacement of one of the *N*-methyl groups of **41** with a fluoroethyl group resulted in a significant loss of SERT affinity (K_i = ~19 nM vs. 0.4 nM for **41**)[241] indicating that functionalizing this position was detrimental to binding. Nevertheless, the *para*-fluorobenzyl derivatives **62** (SERT K_i = ~4 nM) and **63** (SERT K_i = ~510 nM) were prepared and evaluated.[242] As seen from the SERT binding affinities the large *p*-fluorobenzyl group can be tolerated to a certain extent if the nitrogen atom is substituted secondarily (**62**) but replacement of the hydrogen atom with a methyl group (**63**) completely abolished any affinity for the SERT. Biodistribution studies in rats with [^{18}F]**63** showed low brain uptake and low selectivity in SERT-rich brain regions. Placement of the *p*-fluorobenzyl group on the anilino-nitrogen (**64**) produced a compound with moderate SERT affinity (K_i = ~10 nM) and replacement of the *p*-fluorobenzyl group with a *p*-fluorobenzoyl group (**65**) further reduced the SERT affinity (K_i = ~14 nM).[243]

During the search for tropane-based cocaine addiction therapeutics as mentioned in the DAT section above, it was discovered that removal of the *N*-methyl group of a tropane to give a nortropane produced compounds with enhanced SERT and NET affinity.[244] Numerous compounds have been prepared in an attempt to obtain SERT-selective nortropane derivatives [245–251] and several have been radiolabeled with ^{11}C.[235,252–255] The fluoroethyl ester nortropanes 66 and ^{67} (Figure 8) have been reported but, similar to **11**, the affinities for the SERT and DAT were nearly equal.[144]

The results of microPET and HRRT PET imaging in monkeys with the *meta*- and *para*-vinyl iodides [^{18}F]**68** and [^{18}F]**69**, respectively, have recently been reported.[256,257] Both **68** and **69** have a high affinity for the SERT (K_i = 0.43 and 0.08 nM, respectively) but substitution in the *para*-position provides about a 5-fold higher affinity. These differences in binding affinity to the SERT translate into significant differences in the imaging behavior of the compounds. MicroPET imaging with [^{18}F]**68** and [^{18}F]**69** was performed in anesthetized cynomolgus monkeys (Figure 9) and PET imaging on an HRRT with [^{18}F]**68** and [^{18}F]**69** was performed in an awake rhesus monkey (Figure 10). The time required to reach peak uptake is significantly different for the two isomers with the stronger binding *para*-isomer [^{18}F]**69** taking longer to reach peak uptake. Also, the times required for each tracer to reach peak uptake are about the same in both the anesthetized and awake states indicating that anesthesia does not significantly affect the performance of these tracers. After reaching peak uptake the activity of [^{18}F]**68** in the midbrain, putamen, thalamus, medulla, and caudate remains nearly steady for about 20 min followed by a constant washout during which time (65–175 min post-injection) a pseudo-equilibrium is achieved. Compound [^{18}F]**69** takes significantly longer to reach peak uptake in the SERT-rich brain regions and then only slightly washes out. The uptake of [^{18}F]**69** in the cerebellum reaches peak uptake after 45 min followed by a steady washout which provides ever increasing tissue-to-cerebellum ratios as the study progresses. Because the washout of [^{18}F]**68** from the SERT-rich brain regions is nearly parallel to the washout from the cerebellum the tissue-to-cerebellum ratios for [^{18}F]**68** slowly increase throughout the course of the study. Thus, [^{18}F]**68** provides superior imaging kinetics and achieves a pseudo-equilibrium whereas [^{18}F]**69** provides higher uptake ratios. Both of the tracers can be displaced with citalopram but the observed displacement is significantly greater for [^{18}F]**69** because of the minor washout that occurs (under baseline conditions) after peak uptake is achieved which results in only slightly declining time-activity curves. When a citalopram chase is then performed the slope of the time-activity curves of [^{18}F]**69** changes drastically. Thus, each of these tracers is a promising candidate for human use because each has its own unique imaging properties. Compound [^{18}F]**68** can be used for kinetic analysis because of its ability to achieve a pseudo-equilibrium whereas compound [^{18}F]**69** can be used for SSRI occupancy studies due to the large change in slope of the time-activity curves that occurs when an SSRI is administered.

The goal of developing an ^{18}F-radiolabeled PET tracer for imaging the SERT has benefited from the availability of high affinity and selective compounds from both the diphenylsulfide and nortropane classes. Compounds [^{11}C]**42** and [^{11}C]**45** have both demonstrated their utility in imaging normal human volunteers but the adaptation of these compounds to ^{18}F-labeled tracers has so far proven difficult. The ^{18}F-labeled nortropanes [^{18}F]**68** and [^{18}F]**69** have been shown to have improved kinetics relative to their ^{11}C-labeled counterparts, [^{11}C]*m*ZIENT [235] and [^{11}C]*p*ZIENT,[255] respectively, and we look forward to evaluating [^{18}F]**68** and [^{18}F]**69** in healthy human volunteers.

Norepinephrine Transporter (NET)

The human NET is a 617-amino acid transmembrane protein and is 98.9% homologous to the monkey NET.[4,174,258] The NET is found in high densities in the locus coeruleus, cerebellum, dorsal raphe nuclei, thalamus, and hypothalamus.[233,234,239,259,260] The

norepinephrine system has been associated with a variety of neuropsychiatric diseases including PD,[261] ADHD,[262,263] posttraumatic stress disorder (PTSD),[264] depression and anxiety,[240,265–267] and seizure,[268] and a reduction in NET density has been demonstrated postmortem in depressed subjects.[269] The availability of specific and selective NET PET imaging agents will allow for density measurements of the NET and may help to clarify the role of the NET in certain psychiatric diseases as well as help to identify and evaluate NET therapeutics.[270–272]

The antidepressant reboxetine **70** (Figure 11, Table 4) is a selective norepinephrine reuptake inhibitor (SNRI) which is marketed as the racemic mixture.[236,273,274] The ethyl group of **70** has been replaced with a [^{11}C]methyl group to give [^{11}C]**71** and PET imaging comparisons in baboon between *racemic*-[^{11}C]**71**, (*S*,*S*)-[^{11}C]**71**, and (*R*,*R*)-[^{11}C]**71** has shown that (*S*,*S*)-[^{11}C]**71** is the active isomer based on a significantly higher distribution volume in the thalamus and the ability to block the uptake of (*S*,*S*)-[^{11}C]**71**, but not (*R*,*R*)-[^{11}C]**71**, in the thalamus and cerebellum with nisoxetine.[275] The uptake of (*S*,*S*)-[^{11}C]**71** in the striatum could not be blocked with nisoxetine thus demonstrating either low affinity binding or non-specific binding in this brain region. In biodistribution studies in rats (*S*,*S*)-[^{11}C]**71** showed a hypothalamus-to-striatum ratio of 2.5 at 60 min post-injection whereas (*R*,*R*)-[^{11}C]**71** showed only a homogenous distribution.[276] Plasma analysis indicated that (*S*,*S*)-[^{11}C]**71** was metabolized rapidly in the periphery with 50% unmetabolized radiotracer remaining after 30 min and 20% remaining after 60 min but whole rat brain extracts showed that 95% of radioactivity in the brain was unmetabolized (*S*,*S*)-[^{11}C]**71**. PET imaging with (*S*,*S*)-[^{11}C]**71** in cynomolgus monkeys showed the highest uptake in the lower brainstem, mesencephalon, and thalamus while the lowest uptake was in the striatum.[277] Thus, three groups independently verified that (*S*,*S*)-[^{11}C]**71** could be used to image the NET in vivo with PET although specific peak binding equilibrium is not achieved during the course of these studies. Based on these results fluoroalkyl ether derivatives of reboxetine have been developed in pursuit of an ^{18}F-labeled NET PET tracer which would enable longer imaging times and possibly the achievement of peak specific binding equilibrium.

Compound (*S*,*S*)-[^{18}F]**72** is a fluorinated derivative of (*S*,*S*)-[^{11}C]**71** but PET imaging in a cynomolgus monkey with (*S*,*S*)-[^{18}F]**72** showed rapid defluorination and skull uptake. Thus, the deuterated derivative (*S*,*S*)-[^{18}F]**73** was developed and PET imaging showed that defluorination was reduced but not totally inhibited.[278] During PET imaging the total brain uptake of (*S*,*S*)-[^{18}F]**72** peaked at 8 min and then washed out whereas total brain uptake of (*S*,*S*)-[^{18}F]**73** peaked at 12 min and then washed out. The uptake of both (*S*,*S*)-[^{18}F]**72** and (*S*,*S*)-[^{18}F]**73** could be blocked with desipramine but blocking with **1** or citalopram did not have any effect on the uptake of either tracer. At 110 min after injection of (*S*,*S*)-[^{18}F]**72** the tissue-to-striatum ratios were 1.2, 1.2, and 1.3 for the lower brainstem, mesencephalon, and thalamus, respectively. At 160 min after injection of (*S*,*S*)-[^{18}F]**73** the tissue-to-striatum ratios were 1.5, 1.6, 1.3, and 1.5 for the lower brainstem, mesencephalon, thalamus, and temporal cortex, respectively. Peak specific binding was achieved at 90–120 min for (*S*,*S*)-[^{18}F]**72** and at 120–160 min for (*S*,*S*)-[^{18}F]**73**. Autoradiography with (*S*,*S*)-[^{18}F]**73** using post-mortem human brain slices showed the highest accumulation of radioactivity in the locus coeruleus with lower accumulation in the cerebellum, cortex, thalamus, and hypothalamus along with non-specific binding in the caudate nucleus and putamen.[279] A low signal-to-noise ratio was seen outside the locus coeruleus and the authors suggest that the binding affinity of (*S*,*S*)-[^{18}F]**73** (K_i = 3.1 nM) may not be sufficient enough for visualization and quantification of the NET in low density regions. Biodistribution and radiation dosimetry studies have been performed with (*S*,*S*)-[^{18}F]**73** in cynomolgus monkeys[280] and humans[281] and (*S*,*S*)-[^{18}F]**73** has been used to measure the occupancy of the SNRI atomoxetine.[282] Initial human imaging studies with (*S*,*S*)-[^{18}F]**73** have recently been reported.[283] Using 4 healthy male subjects the mean peak uptake in the whole brain was 2.6 ± 0.5% at 12.5 min after injection. Uptake in the

thalamus achieved peak equilibrium with a thalamus-to-caudate ratio of 1.5. Cortical uptake was high due to high skull uptake resulting from defluorination. Thus, (*S*,*S*)-[^{18}F]**73** is a promising PET tracer for imaging the NET in humans but the inability to totally stop defluorination suggests that further structural improvements are still needed.

Compound **74** is a fluorinated derivative of **70** and compound **75** is the deuterated analog of **74**, the deuteration strategy again being employed to inhibit defluorination.[284] Biodistribution studies in mice with (*S*,*S*)-[^{18}F]**74** and (*S*,*S*)-[^{18}F]**75** showed high accumulation of both tracers in the kidneys, liver, and intestines. Brain uptake was moderate and washout was slow for both (*S*,*S*)-[^{18}F]**74** and (*S*,*S*)-[^{18}F]**75**. At 2 h post-injection the average bone uptake of (*S*,*S*)-[^{18}F]**74** was 0.83% ID/g and that of (*S*,*S*)-[^{18}F]**75** was 0.25% ID/g thus demonstrating a reduction of defluorination via the deuterium isotope effect. A PET imaging comparison in baboons with (*S*,*S*)-[^{11}C]**71** and (*S*,*S*)-[^{18}F]**75** (along with several other ^{11}C-labeled NET ligands) determined that (*S*,*S*)-[^{11}C]**71** still has the best PET imaging characteristics of the prospective NET PET tracers available at that time due to the higher signal-to-noise ratio obtained with (*S*,*S*)-[^{11}C]**71** and its faster washout from the striatum.[271,285]

Compounds **76**–**81** have recently been developed as potential NET PET tracers.[286,287] Compounds **76**–**79** have directly connected the alkyl group to the aryl ring thereby eliminating the phenyl alkyl ether functionality and thus possibly enhancing the metabolic stability of the radiolabel. Compounds **77**, **80**, and **81** have incorporated a sulfur atom in replacement of the benzyl phenyl ether oxygen atom. Compounds **76** and **77** each have a high affinity for the NET (K_i = 1.02 ± 0.11 and 0.30 ± 0.03 nM, respectively) which is very similar to the NET affinity of **70** (K_i = 1.04 ± 0.16 nM) and **71** (0.95 ± 0.03 nM).[287] Thus, the phenyl methyl ether oxygen atom is not an important determinant of binding affinity at the NET and a slight enhancement in affinity results from replacing the benzyl phenyl ether oxygen atom with a sulfur atom. Compound **77** has an enhanced SERT affinity (K_i = 14.8 ± 2.83 nM) relative to **76** (K_i = 93 ± 20 nM) indicating that the benzyl phenyl ether oxygen atom is necessary for low SERT affinity. Compounds **78** and **79** each had a reduced NET affinity (K_i = 3.14 ± 0.17 and 3.68 ± 0.92 nM, respectively) compared to **76** indicating that larger alkyl groups, or fluorine substitution, or both, is detrimental to the NET affinity of this series of compounds. MicroPET imaging with [^{11}C]**76** in an anesthetized rhesus monkey showed peak uptake around 20 min followed by a steady washout with tissue-to-caudate ratios of 1.30, 1.45, 1.40, and 1.30 at 45 min post-injection and 1.30, 1.43, 1.44, and 1.25 at 85 min post-injection for the thalamus, midbrain, pons, and cerebellum, respectively, indicating that a quasi-equilibrium had been achieved. MicroPET imaging with [^{11}C]**77** in an anesthetized rhesus monkey showed peak uptake around 30–40 min followed by a steady washout (but slower than that of [^{11}C]**76**) with a thalamus-to-caudate ratio of 1.34 and a midbrain-to-caudate ratio of 1.33 at 85 min post-injection. Because of the moderate affinity **77** has for the SERT, a chase study was performed with (*R*,*S*)-citalopram•HBr (1.5 mg/kg) at 40 min post-injection. The uptake of radioactivity in the caudate did not change indicating that this uptake was most likely the result of nonspecific binding rather than SERT binding. PET imaging on an HRRT was performed in awake rhesus monkeys with [^{11}C]**76** and [^{11}C]**77** to assess the effects of anesthesia on the performance of these tracers. With [^{11}C]**76** high uptake was observed in the thalamus, locus coeruleus, midbrain, and pons and the kinetics were very similar to that observed in the microPET study with an anesthetized rhesus monkey but the tissue-to-caudate ratios were slightly reduced in the awake state. Compound [^{11}C]**77**, on the other hand, showed significantly different kinetics than that observed in the microPET study with an anesthetized rhesus monkey with prolonged retention observed over the course of the study and very little washout. The tissue-to-caudate ratios were also slightly reduced in the awake state. It is known that the anesthetic ketamine (which is used to initially anesthetize the animal before administration of isoflurane) binds to the NET[288] and this may be the cause of the differences observed between the anesthetized and awake states. In microPET studies with [^{18}F]**78** and [^{18}F]**79** in anesthetized rhesus

monkeys peak uptake was achieved in all regions of interest after 15 min followed by a fast washout. High uptake was also observed in the caudate with tissue-to-caudate ratios for the thalamus, midbrain, and cerebellum of 1.13, 1.13, and 1.05, respectively, for [^{18}F]**78** and 1.18, 1.18, and 0.95, respectively, for [^{18}F]**79**. Thus, the poor performance of [^{18}F]**78** and [^{18}F]**79** eliminates them as potential ^{18}F-labeled NET PET tracers.

As mentioned in the DAT section above, cocaine binds to the NET and numerous tropane derivatives have been reported as ligands for the NET.[289–294] Preliminary microPET evaluation of a ^{11}C-labeled NET tropane derivative showed both SERT and NET binding and, therefore, a lack of NET selectivity.[295] The NET ligands talopram[296] and talsupram have been radiolabeled with ^{11}C and evaluated with PET but neither compound entered the brain in sufficient amounts to become a viable PET tracer.[297]

The goal of developing an ^{18}F-labeled PET tracer for the NET is still a work-in-progress but progress is indeed being made. The results above with reboxetine derivatives demonstrate that some minor structural variation can be tolerated without a significant loss in NET affinity but it appears that placing an ^{18}F-radiolabel on the methoxy or ethoxy group does reduce the NET affinity. A similar loss in affinity was observed when going from **35** to **36**. Furthermore, defluorination also is a problem that can only be reduced, but not stopped, by incorporation of deuterium into these fluoroalkoxy groups. Defluorination was also observed with [^{18}F]**36** which, in combination with the ^{18}F-NET ligand data above, suggests that radiolabeling with [^{18}F]methyl and [^{18}F]ethyl ethers and thioethers should be avoided if at all possible. Thus, the development of a reboxetine-based ^{18}F-labeled PET tracer for the NET may require that the ^{18}F-radiolabel be placed on one of the aromatic rings.

Summary

Progress is being made towards the development of fluorine-18 radiolabeled PET tracers for the DAT, SERT, and NET. The greatest number of potential tracers developed so far has been for the DAT due to the greater number of years that have been devoted to this target but also due in part to the concurrent research effort focused on developing a cocaine addiction therapeutic based on the tropane skeleton. The development of a library of potential therapeutic tropane compounds with high DAT affinity that could be radiolabeled with ^{11}C aided in the discovery of PET tracers for the DAT as well as the SERT, and this knowledge was then successfully translated to ^{18}F-labeled tropane derivatives for both the DAT and SERT. The diphenylsulfide class of SERT ligands has already found success with ^{11}C-labeled PET tracers and a viable ^{18}F-labeled PET tracer may soon be realized. Fewer tracers for the NET have been reported because PET imaging of the NET has received considerable less attention than the DAT or SERT but promising, though not optimal, compounds have already been reported. Further work towards this goal should also eventually provide a viable ^{18}F-labeled NET PET tracer.

It is very difficult to predict if a proposed compound will have the desired properties of a PET tracer and so numerous compounds generally have to be synthesized and evaluated. As demonstrated with [^{18}F]**1**-[^{18}F]**4**, [^{18}F]**34**, and [^{11}C]**35**, radiolabeling an antidepressant will not necessarily produce a good PET tracer. On the other hand, derivatives of antidepressants may produce candidate PET tracers as evidenced by the derivatives of **40** shown in Figure 6 and Table 3 and the derivatives of **70** shown in Figure 11 and Table 4. A high binding affinity to the target and a selectivity for that target are the first requirements that need to be met and any compound that cannot meet these requirements will most likely not succeed. Compounds with a high binding affinity and selectivity must also have a lipophilicity in the range of log*P* = ~1–3 or they will also fail. Furthermore, compounds which appear to have the appropriate affinity, selectivity, and lipophilicity can still fail due to poor kinetics or problems

resulting from metabolism. Thus, the development of suitable PET tracers for the DAT, SERT, and NET is not an easy task, but with continued hard work by many research groups the goal will eventually be realized. It should, in fact, be possible to develop more than one tracer for each target and, as shown above, this has already been done. Which of the available tracers is the "best" would then have to be determined from side-by-side comparisons in the same subject under the same conditions (preferably in a conscious state) while taking into consideration the influence of metabolites that are generated from each individual tracer. This has already been done with many of the tracers reported above and this should continue to be done as part of tracer development. Because the goals of different studies of the same target may vary, the availability of several different tracers with slightly different properties may be of greater benefit to the PET imaging community than having only one "best" tracer for a given target.

References

1. Rudnick G, Clark J. From Synapse to Vesicle: the Reuptake and Storage of Biogenic Amine Neurotransmitters. Biochim. Biophys. Acta 1993;1144:249–263. [PubMed: 8104483]
2. Nelson N. The Family of Na^+/Cl^- Neurotransmitter Transporters. J. Neurochem 1998;71:1785–1803. [PubMed: 9798903]
3. Eisenhofer G. The Role of Neuronal and Extraneuronal Plasma Membrane Transporters in the Inactivation of Peripheral Catecholamines. Pharmacol. Therap 2001;91:35–62. [PubMed: 11707293]
4. Miller GM, Yatin SM, De La Garza R, et al. Cloning of Dopamine, Norepinephrine and Serotonin Transporters from Monkey Brain: Relevance to Cocaine Sensitivity. Mol. Brain Res 2001;87:124–143. [PubMed: 11223167]
5. Gainetdinov RR, Caron MG. Monoamine Transporters: From Genes to Behavior. Annu. Rev. Pharmacol. Toxicol 2003;43:261–284. [PubMed: 12359863]
6. Torres GE, Gainetdinov RR, Caron MG. Plasma Membrane Monoamine Transporters: Structure, Regulation and Function. Nature Reviews Neuroscience 2003;4:13–25.
7. Lester HA, Cao Y, Mager S. Listening to Neurotransmitter Transporters. Neuron 1996;17:807–810. [PubMed: 8938113]
8. Melikian HE. Neurotransmitter Transporter Trafficking: Endocytosis, Recycling, and Regulation. Pharmacol. Therap 2004;104:17–27. [PubMed: 15500906]
9. Iversen L. Neurotransmitter Transporters: Fruitful Targets for CNS Drug Discovery. Mol. Psychiatry 2000;5:357–362. [PubMed: 10889545]
10. Carroll FI, Howell LL, Kuhar MJ. Pharmacotherapies for Treatment of Cocaine Abuse: Preclinical Aspects. J. Med. Chem 1999;42:2721–2736. [PubMed: 10425082]
11. Carroll FI. 2002 Medicinal Chemistry Division Award Address: Monoamine Transporters and Opioid Receptors. Targets for Addiction Therapy. J. Med. Chem 2003;46:1775–1794. [PubMed: 12723940]
12. Volkow ND, Fowler JS, Gatley SJ, et al. PET Evaluation of the Dopamine System of the Human Brain. J. Nucl. Med 1996;37:1242–1256. [PubMed: 8965206]
13. Laakso A, Hietala J. PET Studies of Brain Monoamine Transporters. Curr. Pharm. Des 2000;6:1611–1623. [PubMed: 10974156]
14. Jaffer FA, Weissleder R. Molecular Imaging in the Clinical Arena. JAMA 2005;293:855–862. [PubMed: 15713776]
15. Hammoud DA, Hoffman JM, Pomper MG. Molecular Neuroimaging: From Conventional to Emerging Techniques. Radiology 2007;245:21–42. [PubMed: 17885179]
16. Meyer JH. Imaging the Serotonin Transporter During Major Depressive Disorder and Antidepressant Treatment. J. Psychiatry Neurosci 2007;32:86–102. [PubMed: 17353938]
17. Brooks DJ. Neuroimaging in Parkinson's Disease. NeuroRx 2004;1:243–254. [PubMed: 15717025]
18. Aboagye EO, Price PM, Jones T. In Vivo Pharmacokinetics and Pharmacodynamics in Drug Development Using Positron-Emission Tomography. Drug Discovery Today 2001;6:293–302. [PubMed: 11257581]
19. Laruelle M, Slifstein M, Huang Y. Positron Emission Tomography: Imaging and Quantification of Neurotransporter Availability. Methods 2002;27:287–299. [PubMed: 12183117]

20. Talbot PS, Laruelle M. The Role of In Vivo Molecular Imaging with PET and SPECT in the Elucidation of Psychiatric Drug Action and New Drug Development. Eur. Neuropsychopharmacol 2002;12:503–511. [PubMed: 12468013]
21. Guilloteau D, Chalon S. PET and SPECT Exploration of Central Monoaminergic Transporters for the Development of New Drugs and Treatments in Brain Disorders. Curr. Pharm. Design 2005;11:3237–3245.
22. Lee C-M, Farde L. Using Positron Emission Tomography to Facilitate CNS Drug Development. Trends Pharmacol. Sci 2006;27:310–316. [PubMed: 16678917]
23. Hargreaves RJ. The Role of Molecular Imaging in Drug Discovery and Development. Clin. Pharmacol. Ther 2008;83:349–353. [PubMed: 18167503]
24. Takano A, Suzuki K, Kosaka J, et al. A Dose-Finding Study of Duloxetine Based on Serotonin Transporter Occupancy. Psychopharmacology 2006;185:395–399. [PubMed: 16506079]
25. Schlyer DJ. PET Tracers and Radiochemistry. Ann. Acad. Med. Singapore 2004;33:146–154. [PubMed: 15098627]
26. Ametamey SM, Honer M, Schubiger PA. Molecular Imaging with PET. Chem. Rev 2008;108:1501–1516. [PubMed: 18426240]
27. Miller PW, Long NJ, Vilar R, et al. Synthesis of ^{11}C, ^{18}F,^{15}O, and ^{13}N Radiolabels for Positron Emission Tomography. Angew. Chem. Int. Ed 2008;47:8998–9033.
28. Wernick, MN.; Aarsvold, JN., editors. Emission Tomography: The Fundamentals of PET and SPECT. San Diego, CA, USA; London, UK: Elsevier Academic Press; 2004.
29. Levin CS, Hoffman EJ. Calculation of Positron Range and Its Effect on the Fundamental Limit of Positron Emission Tomography System Spatial Resolution. Phys. Med. Biol 1999;44:781–799. [PubMed: 10211810]
30. Smart BE. Fluorine Substituent Effects (on Bioactivity). J. Fluorine Chem 2001;109:3–11.
31. Böhm H-J, Banner D, Bendels S, et al. Fluorine in Medicinal Chemistry. ChemBioChem 2004;5:637–643. [PubMed: 15122635]
32. DiMagno SG, Sun H. The Strength of Weak Interactions: Aromatic Fluorine in Drug Design. Curr. Top. Med. Chem 2006;6:1473–1482. [PubMed: 16918463]
33. Schweizer E, Hoffmann-Röder A, Schärer K, et al. A Fluorine Scan at the Catalytic Center of Thrombin: C-F, C-OH, and C-OMe Bioisosterism and Fluorine Effects on pK_a and log *D* Values. ChemMedChem 2006;1:611–621. [PubMed: 16892401]
34. Sun S, Adejare A. Fluorinated Molecules as Drugs and Imaging Agents in the CNS. Curr. Med. Top. Chem 2006;6:1457–1464.
35. Müller K, Faeh C, Diederich F. Fluorine in Pharmaceuticals: Looking Beyond Intuition. Science 2007;317:1881–1886. [PubMed: 17901324]
36. Hagmann WK. The Many Roles for Fluorine in Medicinal Chemistry. J. Med. Chem 2008;51:4359–4369. [PubMed: 18570365]
37. Prakash GKS, Hu J. Selective Fluoroalkylations with Fluorinated Sulfones, Sulfoxides, and Sulfides. Acc. Chem. Res 2007;40:921–930. [PubMed: 17708659]
38. Kirk KL. Fluorination in Medicinal Chemistry: Methods, Strategies, and Recent Developments. Org. Proc. Res. Dev 2008;12:305–321.
39. Lasne M-C, Perrio C, Rouden J, et al. Chemistry of β^+-Emitting Compounds Based on Fluorine-18. Top. Curr. Chem 2002;222:201–258.
40. Cai L, Lu S, Pike VW. Chemistry with [^{18}F]Fluoride Ion. Eur. J. Org. Chem 2008:2853–2873.
41. Bejot R, Fowler T, Carroll L, et al. Fluorous Synthesis of ^{18}F Radiotracers with the [^{18}F]Fluoride Ion: Nucleophilic Fluorination as the Detagging Process. Angew. Chem. Int. Ed 2009;48:586–589.
42. Logan J, Fowler JS, Volkow ND, et al. Distribution Volume Ratios Without Blood Sampling from Graphical Analysis of PET Data. J. Cereb. Blood Flow Metab 1996;16:834–840. [PubMed: 8784228]
43. Morris ED, Alpert NM, Fischman AJ. Comparison of Two Compartmental Models for Describing Receptor Ligand Kinetics and Receptor Availability in Multiple Injection PET Studies. J. Cereb. Blood Flow Metab 1996;16:841–853. [PubMed: 8784229]
44. Laruelle M. The Role of Model-Based Methods in the Development of Single Scan Techniques. Nucl. Med. Biol 2000;27:637–642. [PubMed: 11091105]

45. Logan J. Graphical Analysis of PET Data Applied to Reversible and Irreversible Tracers. Nucl. Med. Biol 2000;27:661–670. [PubMed: 11091109]
46. Lammertsma AA. Radioligand Studies:Imaging and Quantitative Analysis. Eur. Neuropsychopharmacol 2002;12:513–516. [PubMed: 12468014]
47. Bentourkia M, Zaidi H. Tracer Kinetic Modeling in PET. PET Clin 2007;2:267–277.
48. Dischino DD, Welch MJ, Kilbourn MR, et al. Relationship Between Lipophilicity and Brain Extraction of C-11-Labeled Radiopharmaceuticals. J. Nucl. Med 1983;24:1030–1038. [PubMed: 6605416]
49. Elfving B, Bjørnholm B, Ebert B, et al. Binding Characteristics of Selective Serotonin Reuptake Inhibitors With Relation to Emission Tomography Studies. Synapse 2001;41:203–211. [PubMed: 11391781]
50. Waterhouse RN. Determination of Lipophilicity and Its Use as a Predictor of Blood-Brain Barrier Penetration of Molecular Imaging Agents. Mol. Imag. Biol 2003;5:376–389.
51. Kilty JE, Lorang D, Amara SG. Cloning and Expression of a Cocaine-Sensitive Rat Dopamine Transporter. Science 1991;254:578–579. [PubMed: 1948035]
52. Shimada S, Kitayama S, Lin C-L, et al. Cloning and Expression of a Cocaine-Sensitive Dopamine Transporter Complementary DNA. Science 1991;254:576–578. [PubMed: 1948034]
53. Giros B, El Mestikawy S, Godinot N, et al. Cloning, Pharmacological Characterization, and Chromosome Assignment of the Human Dopamine Transporter. Mol. Pharmacol 1992;42:383–390. [PubMed: 1406597]
54. Ciliax BJ, Heilman C, Demchyshyn LL, et al. The Dopamine Transporter: Immunochemical Characterization and Localization in Brain. J. Neurosci 1995;15:1714–1723. [PubMed: 7534339]
55. Nirenberg MJ, Vaughan RA, Uhl GR, et al. The Dopamine Transporter is Localized to Dendritic and Axonal Plasma Membranes of Nigrostriatal Dopaminergic Neurons. J. Neurosci 1996;16:436–447. [PubMed: 8551328]
56. Ciliax BJ, Drash GW, Staley JK, et al. Immunocytochemical Localization of the Dopamine Transporter in Human Brain. J. Comp. Neurol 1999;409:38–56. [PubMed: 10363710]
57. Kaufman MJ, Spealman RD, Madras BK. Distribution of Cocaine Recognition Sites in Monkey Brain: I. In Vitro Autoradiography with [^{3}H]CFT. Synapse 1991;9:177–187. [PubMed: 1776130]
58. Niznik HB, Fogel EF, Fassos FF, et al. The Dopamine Transporter Is Absent in Parkinsonian Putamen and Reduced in the Caudate Nucleus. J. Neurochem 1991;56:192–198. [PubMed: 1987318]
59. Chinaglia G, Alvarez FJ, Probst A, et al. Mesostriatal and Mesolimbic Dopamine Uptake Binding Sites are Reduced in Parkinson's Disease and Progressive Supranuclear Palsy: A Quantitative Autoradiographic Study Using [^{3}H]Mazindol. Neuroscience 1992;49:317–327. [PubMed: 1436470]
60. Dawson TM, Dawson VL. Molecular Pathways of Neurodegeneration in Parkinson's Disease. Science 2003;302:819–822. [PubMed: 14593166]
61. Mazei-Robison MS, Couch RS, Shelton RC, et al. Sequence Variation in the Human Dopamine Transporter Gene in Children with Attention Deficit Hyperactivity Disorder. Neuropharmacology 2005;49:724–736. [PubMed: 16171832]
62. Singer HS, Hahn I-H, Moran TH. Abnormal Dopamine Uptake Sites in Postmortem Striatum from Patients with Tourette's Syndrome. Ann. Neurol 1991;30:558–562. [PubMed: 1838678]
63. Marek K, Jennings D, Tamagnan G, et al. Biomarkers for Parkinson's Disease: Tools to Assess Parkinson's Disease Onset and Progression. Ann. Neurol 2008;64:S111–S121. [PubMed: 19127587]
64. Heikkila RE, Manzino L. Behavioral Properties of GBR 12909, GBR 13069 and GBR 13098: Specific Inhibitors of Dopamine Uptake. Eur. J. Pharmacol 1984;103:241–248. [PubMed: 6237922]
65. Andersen PH. The Dopamine Uptake Inhibitor GBR 12909: Selectivity and Molecular Mechanism of Action. Eur. J. Pharmacol 1989;166:493–504. [PubMed: 2530094]
66. Kilbourn MR, Haka MS, Mulholland GK, et al. Regional Brain Distribution of [^{18}F]GBR 13119, a Dopamine Uptake Inhibitor, in CD-1 and C57BL/6 Mice. Eur. J. Pharmacol 1989;166:331–334. [PubMed: 2529129]
67. Ciliax BJ, Kilbourn MR, Haka MS, et al. Imaging the Dopamine Uptake Site with Ex Vivo [^{18}F] GBR 13119 Binding Autoradiography in Rat Brain. J. Neurochem 1990;55:619–623. [PubMed: 2115074]

68. Haka MS, Kilbourn MR. Synthesis of [^{18}F]GBR 12909 for Human Studies of Dopamine Reuptake Sites. J. Nucl. Med 1990;31 Abstract Book Supplement, 901, No. 836.
69. Koeppe RA, Kilbourn MR, Frey KA, et al. Imaging and Kinetic Modeling of [F-18]GBR 12909, A Dopamine Uptake Inhibitor. J. Nucl. Med 1990;31 Abstract Book Supplement, 720, No. 55.
70. Van Dort ME, Chakraborty PK, Wieland DM, et al. Dopamine Uptake Inhibitors: Comparison of ^{125}I- and ^{18}F-Labeled Ligands. J. Nucl. Med 1990;31 Abstract Book Supplement, 898, No. 823.
71. Kilbourn MR, Sherman PS, Pisani T. Repeated Reserpine Administration Reduces In Vivo [^{18}F]GBR 13119 Binding to the Dopamine Uptake Site. Eur. J. Pharmacol 1992;216:109–112. [PubMed: 1526249]
72. Kilbourn MR, Carey JE, Koeppe RA, et al. Biodistribution, Dosimetry, Metabolism and Monkey PET Studies of [^{18}F]GBR 13119. Imaging the Dopamine Uptake System *In Vivo*. Nucl. Med. Biol. (Int. J. Radiat. Appl. Instrum. Part B) 1989;16:569–576.
73. Müller L, Halldin C, Foged C, et al. Synthesis of [^{18}F]NNC 12-0817 and [^{18}F]NNC 12-0818; Two Potential Radioligands for the Dopamine Transporter. Appl. Radiat. Isot 1995;46:323–328. [PubMed: 7581289]
74. Wolf WA, Kuhn DM. Cocaine and Serotonin Neurochemistry. Neurochem. Int 1991;18:33–38.
75. Uhl GR, Hall FS, Sora I. Cocaine, Reward, Movement and Monoamine Transporters. Mol. Psychiatry 2002;7:21–26. [PubMed: 11803442]
76. Ritz MC, Lamb RJ, Goldberg SR, et al. Cocaine Receptors on Dopamine Transporters Are Related to Self-Administration of Cocaine. Science 1987;237:1219–1223. [PubMed: 2820058]
77. Scheffel U, Boja JW, Kuhar MJ. Cocaine Receptors: In Vivo Labeling with ^{3}H-(-)-Cocaine, ^{3}H-WIN 35,065-2, and ^{3}H-WIN 35,428. Synapse 1989;4:390–392. [PubMed: 2603151]
78. Boja JW, Kuhar MJ. [^{3}H]Cocaine Binding and Inhibition of [^{3}H]Dopamine Uptake is Similar in Both the Rat Striatum and Nucleus Accumbens. Eur. J. Pharmacol 1989;173:215–217. [PubMed: 2625137]
79. Fowler JS, Volkow ND, Wolf AP, et al. Mapping Cocaine Binding Sites in Human and Baboon Brain In Vivo. Synapse 1989;4:371–377. [PubMed: 2557686]
80. Fowler JS, Volkow ND, MacGregor RR, et al. Comparative PET Studies of the Kinetics and Distribution of Cocaine and Cocaethylene in Baboon Brain. Synapse 1992;12:220–227. [PubMed: 1481141]
81. Yu D-W, Gatley SJ, Wolf AP, et al. Synthesis of Carbon-11 Labeled Iodinated Cocaine Derivatives and Their Distribution in Baboon Brain Measured Using Positron Emission Tomography. J. Med. Chem 1992;35:2178–2183. [PubMed: 1613745]
82. Gatley SJ, Yu D-W, Fowler JS, et al. Studies with Differentially Labeled [^{11}C]Cocaine, [^{11}C] Norcocaine, [^{11}C]Benzoylecgonine, and [^{11}C]- and 4'-[^{18}F]Fluorococaine to Probe the Extent to Which [^{11}C]Cocaine Metabolites Contribute to PET Images of the Baboon Brain. J. Neurochem 1994;62:1154–1162. [PubMed: 8113802]
83. Kimmel HL, Negus SS, Wilcox KM, et al. Relationship Between Rate of Drug Uptake in Brain and Behavioral Pharmacology of Monoamine Transporter Inhibitors in Rhesus Monkeys. Pharmacol. Biochem. Behavior 2008;90:453–462.
84. Kloss MW, Rosen GM, Rauckman EJ. *N*-Demethylation of Cocaine to Norcocaine. Mol. Pharmacol 1983;23:482–485. [PubMed: 6835204]
85. Jindal SP, Lutz T. Mass Spectrometric Studies of Cocaine Disposition in Animals and Humans Using Stable Isotope-Labeled Analogues. J. Pharm. Sci 1989;78:1009–1014. [PubMed: 2614690]
86. Bergström KA, Halldin C, Kuikka JT, et al. The Metabolite Pattern of [^{123}I]β-CIT Determined with a Gradient HPLC Method. Nucl. Med. Biol 1995;22:971–976. [PubMed: 8998474]
87. Potter PM, Wadkins RM. Carboxylesterases - Detoxifying Enzymes and Targets for Drug Therapy. Curr. Med. Chem 2006;13:1045–1054. [PubMed: 16611083]
88. Lundkvist C, Halldin C, Swahn C-G, et al. Different Brain Radioactivity Curves in a PET Study with [^{11}C]β-CIT Labelled in Two Different Positions. Nucl. Med. Biol 1999;26:343–350. [PubMed: 10382835]
89. Larsen NA, Turner JM, Stevens J, et al. Crystal Structure of a Bacterial Cocaine Esterase. Nature Structural Biology 2002;9:17–21.

90. Clarke RL, Daum SJ, Gambino AJ, et al. Compounds Affecting the Central Nervous System. 4. 3β-Phenyltropane-2-carboxylic Esters and Analogs. J. Med. Chem 1973;16:1260–1267. [PubMed: 4747968]
91. Boja JW, Carroll FI, Rahman MA, et al. New, potent cocaine analogs:ligand binding and transport studies in rat striatum. Eur. J. Pharmacol 1990;184:329–332. [PubMed: 2079102]
92. Carroll FI, Gao Y, Rahman MA, et al. Synthesis, Ligand Binding, QSAR, and CoMFA Study of 3β-(*p*-Substituted phenyl)tropane-2β-carboxylic Acid Methyl Esters. J. Med. Chem 1991;34:2719–2725. [PubMed: 1895292]
93. Carroll FI, Lewin AH, Boja JW, et al. Cocaine Receptor: Biochemical Characterization and Structure-Activity Relationships of Cocaine Analogues at the Dopamine Transporter. J. Med. Chem 1992;35:969–981. [PubMed: 1552510]
94. Kuhar MJ, McGirr KM, Hunter RG, et al. Studies of Selected Phenyltropanes at Monoamine Transporters. Drug Alcohol Dependence 1999;56:9–15.
95. Cook CD, Carroll FI, Beardsley PM. Cocaine-Like Discriminative Stimulus Effects of Novel Cocaine and 3-Phenyltropane Analogs in the Rat. Psychopharmacology 2001;159:58–63. [PubMed: 11797070]
96. Singh S. Chemistry, Design, and Structure-Activity Relationship of Cocaine Antagonists. Chem. Rev 2000;100:925–1024. [PubMed: 11749256]
97. Jin C, Navarro HA, Page K, et al. Synthesis and Monoamine Transporter Binding Properties of 2β-[3′-(substituted benzyl)isoxazol-5-yl]- and 2β-[3′-methyl-4′-(substituted phenyl)isoxazol-5-yl]-3β-(substituted phenyl)tropanes. Bioorg. Med. Chem 2008;16:6682–6688. [PubMed: 18556210]
98. Jin C, Navarro HA, Carroll FI. Development of 3-Phenyltropane Analogues with High Affinity for the Dopamine and Serotonin Transporters and Low Affinity for the Norepinephrine Transporter. J. Med. Chem 2008;51:8048–8056. [PubMed: 19053748]
99. Boja JW, Patel A, Carroll FI, et al. [^{125}I]RTI-55: a potent ligand for dopamine transporters. Eur. J. Pharmacol 1991;194:133–134. [PubMed: 2060590]
100. Meltzer PC, Liang AY, Brownell A-L, et al. Substituted 3-Phenyltropane Analogs of Cocaine: Synthesis, Inhibition of Binding at Cocaine Recognition Sites, and Positron Emission Tomography Imaging. J. Med. Chem 1993;36:855–862. [PubMed: 8464040]
101. Wong DF, Yung B, Dannals RF, et al. In Vivo Imaging of Baboon and Human Dopamine Transporters by Positron Emission Tomography Using [^{11}C]WIN 35,428. Synapse 1993;15:130–142. [PubMed: 8259524]
102. Wilson AA, DaSilva JN, Houle S. *In Vivo* Evaluation of [^{11}C]- and [^{18}F]-Labelled Cocaine Analogues as Potential Dopamine Transporter Ligands for Positron Emission Tomography. Nucl. Med. Biol 1996;23:141–146. [PubMed: 8868286]
103. Farde L, Halldin C, Müller L, et al. PET Study of [^{11}C]β-CIT Binding to Monoamine Transporters in the Monkey and Human Brain. Synapse 1994;16:93–103. [PubMed: 8197578]
104. Någren K, Halldin C, Müller L, et al. Comparison of [^{11}C]Methyl Triflate and [^{11}C]Methyl Iodide in the Synthesis of PET Radioligands such as [^{11}C]β-CIT and [^{11}C]β-CFT. Nucl. Med. Biol 1995;22:965–970. [PubMed: 8998473]
105. Harada N, Ohba H, Fukumoto D, et al. Potential of [^{18}F]β-CFT-FE (2β-Carbomethoxy-3β-(4-fluorophenyl)-8-(2-[^{18}F]fluoroethyl)nortropane) as a Dopamine Transporter Ligand: A PET Study in the Conscious Monkey Brain. Synapse 2004;54:37–45. [PubMed: 15300883]
106. Haaparanta M, Bergman J, Laakso A, et al. [^{18}F]CFT ([^{18}F]WIN 35,428), A Radioligand to Study the Dopamine Transporter With PET: Biodistribution in Rats. Synapse 1996;23:321–327. [PubMed: 8855517]
107. Laakso A, Bergman J, Haaparanta M, et al. [^{18}F]CFT ([^{18}F]WIN 35,428), A Radioligand to Study the Dopamine Transporter With PET: Characterization in Human Subjects. Synapse 1998;28:244–250. [PubMed: 9488509]
108. Rinne JO, Nurmi E, Ruottinen HM, et al. [^{18}F]FDOPA and [^{18}F]CFT Are Both Sensitive PET Markers to Detect Presynaptic Dopaminergic Hypofunction in Early Parkinson's Disease. Synapse 2001;40:193–200. [PubMed: 11304757]

109. Kämäräinen E-L, Kyllönen T, Airaksinen A, et al. Preparation of [^{18}F]β-CFT-FP and [^{11}C]β-CFT-FP, Selective Radioligands for Visualisation of the Dopamine Transporter Using Positron Emission Tomography (PET). J. Labelled Cpd. Radiopharm 2000;43:1235–1244.
110. Koivula T, Marjamäki P, Haaparanta M, et al. Ex Vivo Evaluation of *N*-(3-[^{18}F]fluoropropyl)-2β-carbomethoxy-3β-(4-fluorophenyl)nortropane in Rats. Nucl. Med. Biol 2008;35:177–183. [PubMed: 18312827]
111. Owens MJ, Morgan WN, Plott SJ, et al. Neurotransmitter Receptor and Transporter Binding Profile of Antidepressants and Their Metabolites. J. Pharmacol. Exp. Ther 1997;283:1305–1322. [PubMed: 9400006]
112. Hiemke C, Härtter S. Pharmacokinetics of Selective Serotonin Reuptake Inhibitors. Pharmacol. Therap 2000;85:11–28. [PubMed: 10674711]
113. Neumeyer JL, Tamagnan G, Wang S, et al. *N*-Substituted Analogs of 2β-Carbomethoxy-3β-(4′-iodophenyl)tropane (β-CIT) with Selective Affinity to Dopamine or Serotonin Transporters in Rat Forebrain. J. Med. Chem 1996;39:543–548. [PubMed: 8558525]
114. Neumeyer JL, Wang S, Gao Y, et al. *N*-ω-Fluoroalkyl Analogs of (1*R*)-2β-Carbomethoxy-3β-(4-iodophenyl)-tropane (β-CIT): Radiotracers for Positron Emission Tomography and Single Photon Emission Computed Tomography Imaging of Dopamine Transporters. J. Med. Chem 1994;37:1558–1561. [PubMed: 8201589]
115. Carroll FI, Abraham P, Lewin AH, et al. Isopropyl and Phenyl Esters of 3β-(4-Substituted phenyl) tropan-2β-carboxylic Acids. Potent and Selective Compounds for the Dopamine Transporter. J. Med. Chem 1992;35:2497–2500. [PubMed: 1619622]
116. Baldwin RM, Zea-Ponce Y, Al-Tikriti M, et al. Regional Brain Uptake and Pharmacokinetics of [^{123}I]*N*-ω-Fluoroalkyl-2β-carboxy-3β-(4-iodophenyl)nortropane Esters in Baboons. Nucl. Med. Biol 1995;22:211–219. [PubMed: 7767315]
117. Kuikka JT, Bergström KA, Ahonen A, et al. Comparison of Iodine-123 Labelled 2β-Carbomethoxy-3β-(4-iodophenyl)tropane and 2β-Carbomethoxy-3β-(4-iodophenyl)-*N*-(3-fluoropropyl)nortropane for Imaging of the Dopamine Transporter in the Living Human Brain. Eur. J. Nucl. Med 1995;22:356–360. [PubMed: 7607268]
118. Halldin C, Farde L, Lundkvist C, et al. [^{11}C]β-CIT-FE, a Radioligand for Quantitation of the Dopamine Transporter in the Living Brain Using Positron Emission Tomography. Synapse 1996;22:386–390. [PubMed: 8867033]
119. Lundkvist C, Halldin C, Ginovart N, et al. [^{18}F]β-CIT-FP Is Superior to [^{11}C]β-CIT-FP for Quantitation of the Dopamine Transporter. Nucl. Med. Biol 1997;24:621–627. [PubMed: 9352532]
120. Chaly T, Dhawan V, Kazumata K, et al. Radiosynthesis of [^{18}F] *N*-3-Fluoropropyl-2-β-Carbomethoxy-3-β-(4-Iodophenyl) Nortropane and the First Human Study With Positron Emission Tomography. Nucl. Med. Biol 1996;23:999–1004. [PubMed: 9004288]
121. Kazumata K, Dhawan V, Chaly T, et al. Dopamine Transporter Imaging with Fluorine-18-FPCIT PET. J. Nucl. Med 1998;39:1521–1530. [PubMed: 9744335]
122. Ma Y, Dhawan V, Mentis M, et al. Parametric Mapping of [^{18}F]FPCIT Binding in Early Stage Parkinson's Disease: a PET Study. Synapse 2002;45:125–133. [PubMed: 12112405]
123. Robeson W, Dhawan V, Belakhlef A, et al. Dosimetry of the Dopamine Transporter Radioligand ^{18}F-FPCIT in Human Subjects. J. Nucl. Med 2003;44:961–966. [PubMed: 12791826]
124. Yaqub M, Boellaard R, van Berckel BNM, et al. Quantification of Dopamine Transporter Binding Using [^{18}F]FP-β-CIT and Positron Emission Tomography. J. Cerebral Blood Flow Metab 2007;27:1397–1406.
125. Lee SJ, Oh SJ, Chi DY, et al. One-Step High-Radiochemical-Yield Synthesis of [^{18}F]FP-CIT Using a Protic Solvent System. Nucl. Med. Biol 2007;34:345–351. [PubMed: 17499723]
126. Goodman MM, Keil R, Shoup TM, et al. Fluorine-18-FPCT: A PET Radiotracer for Imaging Dopamine Transporters. J. Nucl. Med 1997;38:119–126. [PubMed: 8998165]
127. Goodman MM, Kilts CD, Keil R, et al. ^{18}F-Labeled FECNT: A Selective Radioligand for PET Imaging of Brain Dopamine Transporters. Nucl. Med. Biol 2000;27:1–12. [PubMed: 10755640]
128. Votaw JR, Howell LL, Martarello L, et al. Measurement of Dopamine Transporter Occupancy for Multiple Injections of Cocaine Using a Single Injection of [F-18]FECNT. Synapse 2002;44:203–210. [PubMed: 11984856]

129. Deterding TA, Votaw JR, Wang CK, et al. Biodistribution and Radiation Dosimetry of the Dopamine Transporter Ligand [^{18}F]FECNT. J. Nucl. Med 2001;42:376–381. [PubMed: 11216538]
130. Tipre DN, Fujita M, Chin FT, et al. Whole-Body Biodistribution and Radiation Dosimetry Estimates for the PET Dopamine Transporter Probe ^{18}F-FECNT in Non-Human Primates. Nucl. Med. Commun 2004;25:737–742. [PubMed: 15208503]
131. Voll RJ, McConathy J, Waldrep MS, et al. Semi-automated Preparation of the Dopamine Transporter Ligand [^{18}F]FECNT for Human PET Imaging Studies. Appl. Radiat. Isot 2005;63:353–361. [PubMed: 15985372]
132. Chen ZP, Wang SP, Li XM, et al. A One-Step Automated High-Radiochemical-Yield Synthesis of ^{18}F-FECNT from Mesylate Precursor. Appl. Radiat. Isot 2008;66:1881–1885. [PubMed: 18571931]
133. Davis MR, Votaw JR, Bremner JD, et al. Initial Human PET Imaging Studies with the Dopamine Transporter Ligand ^{18}F-FECNT. J. Nucl. Med 2003;44:855–861. [PubMed: 12791810]
134. Zoghbi SS, Shetty U, Ichise M, et al. PET Imaging of the Dopamine Transporter with ^{18}F-FECNT: A Polar Radiometabolite Confounds Brain Radioligand Measurements. J. Nucl. Med 2006;47:520–527. [PubMed: 16513622]
135. Cumming P, Yokoi F, Chen A, et al. Pharmacokinetics of Radiotracers in Human Plasma During Positron Emission Tomography. Synapse 1999;34:124–134. [PubMed: 10502311]
136. Gillings NM, Bender D, Falborg L, et al. Kinetics of the Metabolism of Four PET Radioligands in Living Minipigs. Nucl. Med. Biol 2001;28:97–104. [PubMed: 11182570]
137. Greuter HNJM, van Ophemert PLB, Luurtsema G, et al. Optimizing an Online SPE-HPLC Method for Analysis of (*R*)-[^{11}C]1-(2-Chlorophenyl)-*N*-methyl-*N*-(1-methylpropyl)-3-isoquinolinecarboxamide [(*R*)-[^{11}C]PK11195] and its Metabolites in Humans. Nucl. Med. Biol 2005;32:307–312. [PubMed: 15820767]
138. Luurtsema G, Molthoff CFM, Schuit RC, et al. Evaluation of (*R*)-[^{11}C]Verapamil as PET Tracer of P-glycoprotein Function in the Blood-Brain Barrier: Kinetics and Metabolismin in the Rat. Nucl. Med. Biol 2005;32:87–93. [PubMed: 15691665]
139. Shetty HU, Zoghbi SS, Liow J-S, et al. Identification and Regional Distribution in Rat Brain of Radiometabolites of the Dopamine Transporter PET Radioligand[^{11}C]PE2I. Eur. J. Nucl. Med. Mol. Imaging 2007;34:667–678. [PubMed: 17096093]
140. Luurtsema G, Schuit RC, Takkenkamp K, et al. Peripheral Metabolism of [^{18}F]FDDNP and Cerebral Uptake of its Labelled Metabolites. Nucl. Med. Biol 2008;35:869–874. [PubMed: 19026948]
141. Chaly T Jr, Matacchieri R, Dahl R, et al. Radiosynthesis of [^{18}F] *N*-3-Fluoropropyl-2-β-carbomethoxy-3-β(4′ methylphenyl) Nortropane (FPCMT). Appl. Radiat. Isot 1999;51:299–305. [PubMed: 10404612]
142. Chitneni SK, Garreau L, Cleynhens B, et al. Improved Synthesis and Metabolic Stability Analysis of the Dopamine Transporter Ligand [^{18}F]FECT. Nucl. Med. Biol 2008;35:75–82. [PubMed: 18158946]
143. Gu X-H, Zong R, Kula NS, et al. Synthesis and Biological Evaluation of a Series of Novel *N*- or *O*-Fluoroalkyl Derivatives of Tropane: Potential Positron Emission Tomography (PET) Imaging Agents for the Dopamine Transporter. Bioorg. & Med. Chem. Lett 2001;11:3049–3053. [PubMed: 11714608]
144. Peng X, Zhang A, Kula NS, et al. Synthesis and Amine Transporter Affinities of Novel Phenyltropane Derivatives as Potential Positron Emission Tomography (PET) Imaging Agents. Bioorg. & Med. Chem. Lett 2004;14:5635–5639. [PubMed: 15482938]
145. Wuest F, Berndt M, Strobel K, et al. Synthesis and Radiopharmacological Characterization of 2β-carbo-2′-[^{18}F]fluoroethoxy-3β-(4-bromo-phenyl)tropane ([^{18}F]MCL-322) as a PET Radiotracer for Imaging the Dopamine Transporter (DAT). Bioorg. Med. Chem 2007;15:4511–4519. [PubMed: 17467995]
146. Mitterhauser M, Wadsak W, Mien L-K, et al. Synthesis and Biodistribution of [^{18}F]FE@CIT, a New Potential Tracer for the Dopamine Transporter. Synapse 2005;55:73–79. [PubMed: 15529336]
147. Ettlinger DE, Häusler D, Wadsak W, et al. Metabolism and Autoradiographic Evaluation of [^{18}F] FE@CIT: a Comparison with [^{123}I]β-CIT and [^{123}I]FP-CIT. Nucl. Med. Biol 2008;35:475–479. [PubMed: 18482685]

148. Xing D, Chen P, Keil R, et al. Synthesis, Biodistribution, and Primate Imaging of Fluorine-18 Labeled 2β-Carbo-1′-fluoro-2-propoxy-3β-(4-chlorophenyl)tropanes. Ligands for the Imaging of Dopamine Transporters by Positron Emission Tomography. J. Med. Chem 2000;43:639–648. [PubMed: 10691690]

149. Mach RH, Nader MA, Ehrenkaufer RL, et al. Fluorine-18-Labeled Tropane Analogs for PET Imaging Studies of the Dopamine Transporter. Synapse 2000;37:109–117. [PubMed: 10881032]

150. Chen P, Kilts CD, Camp VM, et al. Synthesis, characterization and in vivo evaluation of (*N*-(*E*)-4-[^{18}F]fluorobut-2-en-1-yl)-2β-carbomethoxy-3β-(4-substituted-phenyl)nortropanes for imaging DAT by PET. J. Labelled. Cpd. Radiopharm 1999;42:S400.

151. Goodman MM, Chen P. Fluoroalkenyl Nortropanes. 2000 WO2000064490.

152. Chalon S, Hall H, Saba W, et al. Pharmacological Characterization of (*E*)-*N*-(4-Fluorobut-2-enyl)-2β-carbomethoxy-3β-(4'-tolyl)nortropane (LBT-999) as a Highly Promising Fluorinated Ligand for the Dopamine Transporter. J. Pharmacol. Exp. Ther 2006;317:147–152. [PubMed: 16339913]

153. Dollé F, Emond P, Mavel S, et al. Synthesis,radiosynthesis and in vivo preliminary evaluation of [^{11}C]LBT-999, a selective radioligand for the visualisation of the dopamine transporter with PET. Bioorg. Med. Chem 2006;14:1115–1125. [PubMed: 16219467]

154. Dollé F, Hinnen F, Emond P, et al. Radiosynthesis of [^{18}F]LBT-999, A Selective Radioligand for the Visualization of the Dopamine Transporter with PET. J. Label. Compd. Radiopharm 2006;49:687–698.

155. Dollé F, Helfenbein J, Hinnen F, et al. One-Step Radiosynthesis of [^{18}F]LBT-999: A Selective Radioligand for the Visualization of the Dopamine Transporter with PET. J. Label. Compd. Radiopharm 2007;50:716–723.

156. Saba W, Valette H, Schöllhorn-Peyronneau M-A, et al. [^{11}C]LBT-999: A Suitable Radioligand for Investigation of Extra-Striatal Dopamine Transporter with PET. Synapse 2007;61:17–23. [PubMed: 17068778]

157. Stehouwer, JS.; Chen, P.; Voll, RJ., et al. PET Imaging of the Dopamine Transporter with [^{18}F] FBFNT. J. Labelled. Cpd. Radiopharm; Aachen, Germany. Presented at the 17th International Symposium on Radiopharmaceutical Sciences; 2007. p. S335Poster #248

158. Carroll FI, Kotian P, Dehghani A, et al. Cocaine and 3β-(4′-Substituted phenyl)tropane-2β-carboxylic Acid Ester and Amide Analogues. New High-Affinity and Selective Compounds for the Dopamine Transporter. J. Med. Chem 1995;38:379–388. [PubMed: 7830281]

159. Dworkin SI, Lambert P, Sizemore GM, et al. RTI-113 Administration Reduces Cocaine Self-Administration at High Occupancy of Dopamine Transporter. Synapse 1998;30:49–55. [PubMed: 9704880]

160. Cook CD, Carroll FI, Beardsley PM. RTI 113, a 3-Phenyltropane Analog, Produces Long-Lasting Cocaine-Like Discriminative Stimulus Effects in Rats and Squirrel Monkeys. Eur. J. Pharmacol 2002;442:93–98. [PubMed: 12020686]

161. Wilcox KM, Lindsey KP, Votaw JR, et al. Self-Administration of Cocaine and the Cocaine Analog RTI-113: Relationship to Dopamine Transporter Occupancy Determined by PET Neuroimaging in Rhesus Monkeys. Synapse 2002;43:78–85. [PubMed: 11746736]

162. Tsukada H, Nishiyama S, Kakiuchi T, et al. Isoflurane Anesthesia Enhances the Inhibitory Effects of Cocaine and GBR12909 on Dopamine Transporter: PET Studies in Combination with Microdialysis in the Monkey Brain. Brain Research 1999;849:85–96. [PubMed: 10592290]

163. Miyamoto S, Leipzig JN, Lieberman JA, et al. Effects of Ketamine, MK-801, and Amphetamine on Regional Brain 2-Deoxyglucose Uptake in Freely Moving Mice. Neuropsychopharmacology 2000;22:400–412. [PubMed: 10700659]

164. Tsukada H, Harada N, Nishiyama S, et al. Ketamine Decreased Striatal [^{11}C]Raclopride Binding With No Alterations in Static Dopamine Concentrations in the Striatal Extracellular Fluid in the Monkey Brain: Multiparametric PET Studies Combined With Microdialysis Analysis. Synapse 2000;37:95–103. [PubMed: 10881030]

165. Mizugaki M, Nakagawa N, Nakamura H, et al. Influence of Anesthesia on Brain Distribution of [^{11}C]Methamphetamine in Monkeys in Positron Emission Tomography (PET) Study. Brain Research 2001;911:173–175. [PubMed: 11511387]

166. Tsukada H, Nishiyama S, Kakiuchi T, et al. Ketamine Alters the Availability of Striatal Dopamine Transporter as Measured by [^{11}C]β-CFT and [^{11}C]β-CIT-FE in the Monkey Brain. Synapse 2001;42:273–280. [PubMed: 11746726]

167. Elfving B, Bjørnholm B, Knudsen GM. Interference of Anaesthetics With Radioligand Binding in Neuroreceptor Studies. Eur. J. Nucl. Med. Mol. Imaging 2003;30:912–915. [PubMed: 12715241]

168. Votaw JR, Byas-Smith MG, Voll R, et al. Isoflurane Alters the Amount of Dopamine Transporter Expressed on the Plasma Membrane in Humans. Anesthesiology 2004;101:1128–1135. [PubMed: 15505448]

169. Hoffman BJ, Mezey E, Brownstein MJ. Cloning of a Serotonin Transporter Affected by Antidepressants. Science 1991;254:579–580. [PubMed: 1948036]

170. Cortés R, Soriano E, Pazos A, et al. Autoradiography of Antidepressant Binding Sites in the Human Brain: Localization Using [^{3}H]Imipramine and [^{3}H]Paroxetine. Neuroscience 1988;27:473–496. [PubMed: 2975361]

171. Hrdina PD, Foy B, Hepner A, et al. Antidepressant Binding Sites in Brain: Autoradiographic Comparison of [^{3}H]Paroxetine and [^{3}H]Imipramine Localization and Relationship to Serotonin Transporter. J. Pharmacol. Exp. Ther 1990;252:410–418. [PubMed: 2137177]

172. Fujita M, Shimada S, Maeno H, et al. Cellular Localization of Serotonin Transporter mRNA in the Rat Brain. Neurosci. Lett 1993;162:59–62. [PubMed: 8121638]

173. Austin MC, Bradley CC, Mann JJ, et al. Expression of Serotonin Transporter Messenger RNA in the Human Brain. J. Neurochem 1994;62:2362–2367. [PubMed: 8189241]

174. Blakely RD, De Felice LJ, Hartzell HC. Molecular Physiology of Norepinephrine and Serotonin Transporters. J. Exp. Biol 1994;196:263–281. [PubMed: 7823027]

175. Gurevich EV, Joyce JN. Comparison of [^{3}H]Paroxetine and [^{3}H]Cyanoimipramine for Quantitative Measurement of Serotonin Transporter Sites in Human Brain. Neuropsychopharm 1996;14:309–323.

176. Stockmeier CA, Shapiro LA, Haycock JW, et al. Quantitative Subregional Distribution of Serotonin-1A Receptors and Serotonin Transporters in the Human Dorsal Raphe. Brain Res 1996;727:1–12. [PubMed: 8842377]

177. Kish SJ, Furukawa Y, Chang L-J, et al. Regional Distribution of Serotonin Transporter Protein in Postmortem Human Brain. Is the Cerebellum a SERT-Free Brain Region? Nucl. Med. Biol 2005;32:123–128. [PubMed: 15721757]

178. Chinaglia G, Landwehrmeyer B, Probst A, et al. Serotonergic Terminal Transporters are Differentially Affected in Parkinson's Disease and Progressive Supranuclear Palsy: An Autoradiographic Study with [^{3}H]Citalopram. Neuroscience 1993;54:691–699. [PubMed: 8332256]

179. Cash R, Raisman R, Ploska A, et al. High and Low Affinity [^{3}H]Imipramine Binding Sites in Control and Parkinsonian Brains. Eur. J. Pharmacol 1985;117:71–80. [PubMed: 3002804]

180. Blier P, de Montigny C. Serotonin and Drug-Induced Therapeutic Responses in Major Depression, Obsessive-Compulsive and Panic Disorders. Neuropsychopharm 1999;21:91S–98S.

181. Chaouloff F, Berton O, Mormede P. Serotonin and Stress. Neuropsychopharm 1999;21:28S–32S.

182. Lucki I. The Spectrum of Behaviors Influenced by Serotonin. Biol. Psychiatry 1998;44:151–162. [PubMed: 9693387]

183. Mann JJ. Role of the Serotonergic System in the Pathogenesis of Major Depression and Suicidal Behavior. Neuropsychopharm 1999;21:99S–105S.

184. Mann JJ, Brent DA, Arango V. The Neurobiology and Genetics of Suicide and Attempted Suicide: A Focus on the Serotonergic System. Neuropsychopharm 2001;24:467–477.

185. Owens MJ, Nemeroff CB. Role of Serotonin in the Pathophysiology of Depression: Focus on the Serotonin Transporter. Clin. Chem 1994;40:288–295. [PubMed: 7508830]

186. Owens MJ, Nemeroff CB. The Serotonin Transporter and Depression. Depression and Anxiety 1998;8:5–12. [PubMed: 9809208]

187. Purselle DC, Nemeroff CB. Serotonin Transporter: A Potential Substrate in the Biology of Suicide. Neuropsychopharmacology 2003;28:613–619. [PubMed: 12655305]

188. Benmansour S, Cecchi M, Morilak DA, et al. Effects of Chronic Antidepressant Treatments on Serotonin Transporter Function, Density, and mRNA Level. J. Neurosci 1999;19:10494–10501. [PubMed: 10575045]

189. Benmansour S, Owens WA, Cecchi M, et al. Serotonin Clearance *in vivo* is Altered to a Greater Extent by Antidepressant-Induced Downregulation of the Serotonin Transporter than by Acute Blockade of this Transporter. J. Neurosci 2002;22:6766–6772. [PubMed: 12151556]

190. Ramsey IS, De Felice LJ. Serotonin Transporter Function and Pharmacology Are Sensitive to Expression Level. J. Biol. Chem 2002;277:14475–14482. [PubMed: 11844791]

191. Kugaya A, Sanacora G, Staley JK, et al. Brain Serotonin Transporter Availability Predicts Treatment Response to Selective Serotonin Reuptake Inhibitors. Biol. Psychiatry 2004;56:497–502. [PubMed: 15450785]

192. Mirza NR, Nielsen EØ, Troelsen KB. Serotonin Transporter Density and Anxiolytic-like Effects of Antidepressants in Mice. Prog. Neuro-Psychopharm. Biol. Psych 2007;31:858–866.

193. Stokes PE. Ten Years of Fluoxetine. Depression and Anxiety 1998;8:1–4. [PubMed: 9809207]

194. Shiue C-Y, Shiue GG, Cornish KG, et al. PET Study of the Distribution of [^{11}C]Fluoxetine in a Monkey Brain. Nucl. Med. Biol 1995;22:613–616. [PubMed: 7581171]

195. Mukherjee J, Das MK, Yang Z-Y, et al. Evaluation of the Binding of the Radiolabeled Antidepressant Drug, ^{18}F-Fluoxetine in the Rodent Brain: An *In Vitro* and *In Vivo* Study. Nucl. Med. Biol 1998;25:605–610. [PubMed: 9804041]

196. Shank RP, Vaught JL, Pelley KA, et al. McN-5652: A Highly Potent Inhibitor of Serotonin Uptake. J. Pharmacol. Exp. Ther 1988;247:1032–1038. [PubMed: 2905001]

197. Suehiro M, Scheffel U, Dannals RF, et al. A PET Radiotracer for Studying Serotonin Uptake Sites: Carbon-11-McN-5652Z. J. Nucl. Med 1993;34:120–127. [PubMed: 8418252]

198. Szabo Z, Kao PF, Scheffel U, et al. Positron Emission Tomography Imaging of Serotonin Transporters in the Human Brain Using [^{11}C](+)McN5652. Synapse 1995;20:37–43. [PubMed: 7624828]

199. Zessin J, Eskola O, Brust P, et al. Synthesis of S-([^{18}F]fluoromethyl)-(+)-McN5652 as a Potential PET Radioligand for the Serotonin Transporter. Nucl. Med. Biol 2001;28:857–863. [PubMed: 11578908]

200. Marjamäki P, Zessin J, Eskola O, et al. S-[^{18}F]fluoromethyl-(+)-McN5652, a PET Tracer for the Serotonin Transporter: Evaluation in Rats. Synapse 2003;47:45–53. [PubMed: 12422372]

201. Brust P, Hinz R, Kuwabara H, et al. *In vivo* Measurement of the Serotonin Transporter with (*S*)-([^{18}F]fluoromethyl)-(+)-McN5652. Neuropsychopharmacology 2003;28:2010–2019. [PubMed: 12931143]

202. Brust P, Zessin J, Kuwabara H, et al. Positron Emission Tomography Imaging of the Serotonin Transporter in the Pig Brain Using [^{11}C](+)-McN5652 and S-([^{18}F]fluoromethyl)-(+)-McN5652. Synapse 2003;47:143–151. [PubMed: 12454952]

203. Kretzschmar M, Brust P, Zessin J, et al. Autoradiographic Imaging of the Serotonin Transporter in the Brain of Rats and Pigs Using *S*-([^{18}F]fluoromethyl)-(+)-McN5652. Eur. Neuropsychopharmacol 2003;13:387–397. [PubMed: 12957338]

204. Hashimoto K, Goromaru T. High-Affinity [^{3}H]6-Nitroquipazine Binding Sites in Rat Brain. Eur. J. Pharmacol 1990;180:273–281. [PubMed: 1694774]

205. Karramkam M, Dollé F, Valette H, et al. Synthesis of a Fluorine-18-labelled Derivative of 6-Nitroquipazine as a Radioligand for the In Vivo Serotonin Transporter Imaging with PET. Bioorg. Med. Chem 2002;10:2611–2623. [PubMed: 12057650]

206. Lee BS, Chu S, Lee KC, et al. Syntheses and Binding Affinities of 6-Nitroquipazine Analogues for Serotonin Transporter: Part 3. A Potential 5-HT Transporter Imaging Agent,3-(3-[^{18}F] Fluoropropyl)-6-nitroquipazine. Bioorg. Med. Chem 2003;11:4949–4958. [PubMed: 14604657]

207. Mehta, NB.; Hollingsworth, CEB.; Brieaddy, LE., et al. Halogen Substituted Diphenylsulfides. European Patent Application. 0 402 097 A401. 1990.

208. Ferris RM, Brieaddy L, Mehta N, et al. Pharmacological Properties of 403U76, a New Chemical Class of 5-Hydroxytryptamine-and Noradrenaline-reuptake Inhibitor. J. Pharm. Pharmacol 1995;47:775–781. [PubMed: 8583392]

209. Oya S, Choi SR, Hou C, et al. 2-((2-((Dimethylamino)methyl)phenyl)thio)-5-iodophenylamine (ADAM): An Improved Serotonin Transporter Ligand. Nucl. Med. Biol 2000;27:249–254. [PubMed: 10832081]

210. Houle S, Ginovart N, Hussey D, et al. Imaging the Serotonin Transporter with Positron Emission Tomography: Initial Human Studies with [^{11}C]DAPP and [^{11}C]DASB. Eur. J. Nucl. Med 2000;27:1719–1722. [PubMed: 11105830]

211. Wilson AA, Ginovart N, Schmidt M, et al. Novel Radiotracers for Imaging the Serotonin Transporter by Positron Emission Tomography: Synthesis, Radiosynthesis, and in Vitro and ex Vivo Evaluation of ^{11}C-Labeled 2-(Phenylthio)araalkylamines. J. Med. Chem 2000;43:3103–3110. [PubMed: 10956218]

212. Ginovart N, Wilson AA, Meyer JH, et al. Positron Emission Tomography Quantification of [^{11}C]-DASB Binding to the Human Serotonin Transporter: Modeling Strategies. J. Cereb. Blood Flow Metab 2001;21:1342–1353. [PubMed: 11702049]

213. Huang Y, Hwang D-R, Narendran R, et al. Comparative Evaluation in Nonhuman Primates of Five PET Radiotracers for Imaging the Serotonin Transporters: [^{11}C]McN5652, [^{11}C]ADAM, [^{11}C] DASB, [^{11}C]DAPA, and [^{11}C]AFM. J Cereb Blood Flow Metab 2002;22:1377–1398. [PubMed: 12439295]

214. Huang Y, Hwang D-R, Bae S, et al. A New Positron Emission Tomography Imaging Agent for the Serotonin Transporter: Synthesis, Pharmacological Characterization, and Kinetic Analysis of [^{11}C]2-[2-(dimethylaminomethyl)phenylthio]-5-fluoromethylphenylamine ([^{11}C]AFM). Nucl. Med. Biol 2004;31:543–556. [PubMed: 15219271]

215. Huang Y, Narendran R, Bae S, et al. A PET Imaging Agent with Fast Kinetics: Synthesis and In Vivo Evaluation of the Serotonin Transporter Ligand [^{11}C]2-[2-dimethylaminomethylphenylthio)]-5-fluorophenylamine ([^{11}C]AFA). Nucl. Med. Biol 2004;31:727–738. [PubMed: 15246363]

216. Zhu Z, Guo N, Narendran R, et al. The New PET Imaging Agent [^{11}C]AFE is a Selective Serotonin Transporter Ligand with Fast Brain Uptake Kinetics. Nucl. Med. Biol 2004;31:983–994. [PubMed: 15607480]

217. Jarkas N, McConathy J, Votaw JR, et al. Synthesis and Characterization of EADAM: A Selective Radioligand for Mapping the Brain Serotonin Transporters by Positron Emission Tomography. Nucl. Med. Biol 2005;32:75–86. [PubMed: 15691664]

218. Jarkas N, Votaw JR, Voll RJ, et al. Carbon-11 HOMADAM: A Novel PET Radiotracer for Imaging Serotonin Transporters. Nucl. Med. Biol 2005;32:211–224. [PubMed: 15820756]

219. Frankle WG, Huang Y, Hwang D-R, et al. Comparative Evaluation of Serotonin Transporter Radioligands ^{11}C-DASB and ^{11}C-McN 5652 in Healthy Humans. J. Nucl. Med 2004;45:682–694. [PubMed: 15073266]

220. Frankle WG, Narendran R, Huang Y, et al. Serotonin Transporter Availability in Patients with Schizophrenia: A Positron Emission Tomography Imaging Study with [^{11}C]DASB. Biol. Psychiatry 2005;57:1510–1516. [PubMed: 15953487]

221. Nye JA, Votaw JR, Jarkas N, et al. Compartmental Modeling of ^{11}C-HOMADAM Binding to the Serotonin Transporter in the Healthy Human Brain. J. Nucl. Med 2008;49:2018–2025. [PubMed: 19038997]

222. Shiue GG, Choi S-R, Fang P, et al. *N*,*N*-Dimethyl-2-(2-Amino-4-^{18}F-Fluorophenylthio)-Benzylamine (4-^{18}F-ADAM): An Improved PET Radioligand for Serotonin Transporters. J. Nucl. Med 2003;44:1890–1897. [PubMed: 14660713]

223. Huang Y, Bae S, Zhu Z, et al. Fluorinated Diaryl Sulfides as Serotonin Transporter Ligands: Synthesis, Structure-Activity Relationship Study, and in Vivo Evaluation of Fluorine-18-Labeled Compounds as PET Imaging Agents. J. Med. Chem 2005;48:2559–2570. [PubMed: 15801845]

224. Oya S, Choi SR, Hou C, et al. ^{18}F(2-[2-Amino-5-fluorophenyl)thio]-*N*,*N*-dimethyl-benzenmethanamine) as a PET Imaging Agent for Serotonin Transporters. J. Label. Compd. Radiopharm 2003;46:S164.

225. Oya S, Choi SR, Coenen H, et al. New PET Imaging Agent for the Serotonin Transporter: [^{18}F] ACF (2-[(2-Amino-4-chloro-5-fluorophenyl)thio]-*N*,*N*-dimethyl-benzenmethanamine). J. Med. Chem 2002;45:4716–4723. [PubMed: 12361398]

226. Parhi AK, Wang JL, Oya S, et al. 2-(2'-((Dimethylamino)methyl)-4'-(fluoroalkoxy)-phenylthio) benzenamine Derivatives as Serotonin Transporter Imaging Agents. J. Med. Chem 2007;50:6673–6684. [PubMed: 18052090]

227. Jarkas N, Voll RJ, Williams L, et al. Synthesis and In Vivo Evaluation of Halogenated *N*,*N*-Dimethyl-2-(2′-amino-4′-hydroxymethylphenylthio)benzylamine Derivatives as PET Serotonin Transporter Ligands. J. Med. Chem 2008;51:271–281. [PubMed: 18085744]

228. Huang Y, Zhu Z, Bae S-A, et al. Comparison of Three F-18 Labeled PET Ligands for the Serotonin Transporter: Radiosynthesis and In Vivo Imaging Studies in Baboon. J. Label. Compd. Radiopharm 2003;46:S57.

229. Fang P, Shiue GG, Shimazu T, et al. Synthesis and Evaluation of *N*,*N*-Dimethyl-2-(2-amino-5-[^{18}F]fluorophenylthio)benzylamine (5-[^{18}F]-ADAM) as a Serotonin Transporter Imaging Agent. Appl. Radiat. Isot 2004;61:1247–1254. [PubMed: 15388117]

230. Wang JL, Parhi AK, Oya S, et al. 2-(2′-((Dimethylamino)methyl)-4′-(3-[^{18}F]fluoropropoxy)-phenylthio)benzenamine for Positron Emission Tomography Imaging of Serotonin Transporters. Nucl. Med. Biol 2008;35:447–458. [PubMed: 18482682]

231. Owens MJ, Knight DL, Nemeroff CB. Second-Generation SSRIs: Human Monoamine Transporter Binding Profile of Escitalopram and *R*-Fluoxetine. Biol. Psychiatry 2001;50:345–350. [PubMed: 11543737]

232. Elfving B, Wiborg O. Binding of S-Citalopram and Paroxetine Discriminates Between Species. Synapse 2005;55:280–282. [PubMed: 15668984]

233. Tejani-Butt SM. [^{3}H]Nisoxetine: A Radioligand for Quantitation of Norepinephrine Uptake Sites by Autoradiography or by Homogenate Binding. J. Pharmacol. Exp. Ther 1992;260:427–436. [PubMed: 1731049]

234. Cheetham SC, Viggers JA, Butler SA, et al. [^{3}H]Nisoxetine - A Radioligand for Noradrenaline Reuptake Sites: Correlation With Inhibition of [^{3}H]Noradrenaline Uptake and Effects of DSP-4 Lesioning and Antidepressant Treatments. Neuropharmacology 1996;35:63–70. [PubMed: 8684598]

235. Stehouwer JS, Jarkas N, Zeng F, et al. Synthesis, Radiosynthesis, and Biological Evaluation of Carbon-11 Labeled 2β-Carbomethoxy-3β-(3′-((Z)-2-haloethenyl)phenyl)nortropanes: Candidate Radioligands for In Vivo Imaging of the Serotonin Transporter with Positron Emission Tomography. J. Med. Chem 2006;49:6760–6767. [PubMed: 17154506]

236. Wong EHF, Sonders MS, Amara SG, et al. Reboxetine: A Pharmacologically Potent, Selective, and Specific Norepinephrine Reuptake Inhibitor. Biol. Psychiatry 2000;47:818–829. [PubMed: 10812041]

237. Goodman MM, Chen P, Plisson C, et al. Synthesis and Characterization of Iodine-123 Labeled 2β-Carbomethoxy-3β-(4′-((Z)-2-iodoethenyl)phenyl)nortropane. A Ligand for *in vivo* Imaging of Serotonin Transporters by Single-Photon-Emission Tomography. J. Med. Chem 2003;46:925–935. [PubMed: 12620070]

238. Plaznik A, Danysz W, Kostowski W, et al. Interaction Between Noradrenergic and Serotonergic Brain Systems as Evidenced by Behavioral and Biochemical Effects of Microinjections of Adrenergic Agonists and Antagonists into the Medial Raphe Nucleus. Pharmacol. Biochem. Behavior 1983;19:27–32.

239. Ordway GA, Stockmeier CA, Cason GW, et al. Pharmacology and Distribution of Norepinephrine Transporters in the Human Locus Coeruleus and Raphe Nuclei. J. Neurosci 1997;17:1710–1719. [PubMed: 9030630]

240. Ressler KJ, Nemeroff CB. Role of Serotonergic and Noradrenergic Systems in the Pathophysiology of Depression and Anxiety Disorders. Depression and Anxiety 2000;12:2–19. [PubMed: 11098410]

241. Emond P, Vercouillie J, Innis R, et al. Substituted Diphenyl Sulfides as Selective Serotonin Transporter Ligands: Synthesis and In Vitro Evaluation. J. Med. Chem 2002;45:1253–1258. [PubMed: 11881994]

242. Garg S, Thopate SR, Minton RC, et al. 3-Amino-4-(2-((4-[^{18}F]fluorobenzyl)methylamino) methylphenylsulfanyl)benzonitrile, an F-18 Fluorobenzyl Analogue of DASB: Synthesis, *in Vitro* Binding, and *in Vivo* Biodistribution Studies. Bioconj. Chem 2007;18:1612–1618.

243. Mavel S, Vercouillie J, Garreau L, et al. Docking Study, Synthesis, and In Vitro Evaluation of Fluoro-MADAM Derivatives as SERT Ligands for PET Imaging. Bioorg. Med. Chem 2008;16:9050–9055. [PubMed: 18793858]

244. Boja JW, Kuhar MJ, Kopajtic T, et al. Secondary Amine Analogues of 3β-(4′-Substituted phenyl) tropane-2β-carboxylic Acid Esters and *N*-Norcocaine Exhibit Enhanced Affinity for Serotonin and Norepinephrine Transporters. J. Med. Chem 1994;37:1220–1223. [PubMed: 8164265]

245. Blough BE, Abraham P, Lewin AH, et al. Synthesis and Transporter Binding Properties of 3β-(4′-Alkyl-, 4′-alkenyl-, and 4′-alkynylphenyl)nortropane-2β-carboxylic Acid Methyl Esters: Serotonin Transporter Selective Analogs. J. Med. Chem 1996;39:4027–4035. [PubMed: 8831768]

246. Blough BE, Abraham P, Mills AC, et al. 3β-(4-Ethyl-3-iodophenyl)nortropane-2β-carboxylic Acid Methyl Ester as a High-Affinity Selective Ligand for the Serotonin Transporter. J. Med. Chem 1997;40:3861–3864. [PubMed: 9397165]

247. Tamagnan G, Baldwin RM, Kula NS, et al. Synthesis and Monoamine Transporter Affinity of 2β-Carbomethoxy-3β-(2″-, 3″- or 4″-substituted) Biphenyltropanes. Bioorg. & Med. Chem. Lett 2000;10:1783–1785. [PubMed: 10969967]

248. Emond P, Helfenbein J, Chalon S, et al. Synthesis of Tropane and Nortropane Analogues with Phenyl Substitutions as Serotonin Transporter Ligands. Bioorg. & Med. Chem 2001;9:1849–1855. [PubMed: 11425587]

249. Bois F, Baldwin RM, Kula NS, et al. Synthesis and Monoamine Transporter Affinity of 3′-Analogs of 2-β-Carbomethoxy-3-β-(4′-iodophenyl)tropane (β-CIT). Bioorg. & Med. Chem. Lett 2004;14:2117–2120. [PubMed: 15080991]

250. Tamagnan G, Alagille D, Fu X, et al. Synthesis and Monoamine Transporter Affinity of New 2β-Carbomethoxy-3β-[4-(Substituted Thiophenyl)]Phenyltropanes: Discovery of a Selective SERT Antagonist with Picomolar Potency. Bioorg. & Med. Chem. Lett 2005;15:1131–1133. [PubMed: 15686927]

251. Tamagnan G, Alagille D, Fu X, et al. Synthesis and Monoamine Transporter Affinity of New 2β-Carbomethoxy-3β-[aryl or heteroaryl]phenyltropanes. Bioorg. Med. Chem. Lett 2006;16:217–220. [PubMed: 16236497]

252. Bergström KA, Halldin C, Hall H, et al. In Vitro and In Vivo Characterisation of Nor-β-CIT: A Potential Radioligand for Visualisation of the Serotonin Transporter in the Brain. Eur. J. Nucl. Med 1997;24:596–601. [PubMed: 9169564]

253. Helfenbein J, Sandell J, Halldin C, et al. PET Examination of Three Potent Cocaine Derivatives as Specific Radioligands for the Serotonin Transporter. Nucl. Med. Biol 1999;26:491–499. [PubMed: 10473187]

254. Stehouwer JS, Plisson C, Jarkas N, et al. Synthesis, Radiosynthesis, and Biological Evaluation of Carbon-11 and Fluorine-18 (*N*-Fluoroalkyl) Labeled 2β-Carbomethoxy-3β-(4′-(3-furyl)phenyl)-tropanes and -nortropanes: Candidate Radioligands for in Vivo Imaging of the Serotonin Transporter with Positron Emission Tomography. J. Med. Chem 2005;48:7080–7083. [PubMed: 16250668]

255. Plisson C, Jarkas N, McConathy J, et al. Evaluation of Carbon-11-Labeled 2β-Carbomethoxy-3β-[4′-((Z)-2-iodoethenyl)phenyl]nortropane as a Potential Radioligand for Imaging the Serotonin Transporter by PET. J. Med. Chem 2006;49:942–946. [PubMed: 16451060]

256. Plisson C, Stehouwer JS, Voll RJ, et al. Synthesis and *In Vivo* Evaluation of Fluorine-18 and Iodine-123 Labeled 2β-Carbo(2-fluoroethoxy)-3β-(4′-((*Z*)-2-iodoethenyl)phenyl)nortropane as a Candidate Serotonin Transporter Imaging Agent. J. Med. Chem 2007;50:4553–4560. [PubMed: 17705359]

257. Stehouwer JS, Jarkas N, Zeng F, et al. Synthesis, Radiosynthesis, and Biological Evaluation of Fluorine-18-Labeled 2β-Carbo(fluoroalkoxy)-3β-(3′-((*Z*)-2-haloethenyl)phenyl)nortropanes: Candidate Radioligands for In Vivo Imaging of the Serotonin Transporter with Positron Tomography. J. Med. Chem 2008;51:7788–7799. [PubMed: 19053782]

258. Pacholczyk T, Blakely RD, Amara SG. Expression Cloning of a Cocaine- and Antidepressant-Sensitive Human Noradrenaline Transporter. Nature 1991;350:350–354. [PubMed: 2008212]

259. Schroeter S, Apparsundaram S, Wiley RG, et al. Immunolocalization of the Cocaine-and Antidepressant-Sensitive 1-Norepinephrine Transporter. J. Comp. Neurol 2000;420:211–232. [PubMed: 10753308]

260. Sara SJ. The Locus Coeruleus and Noradrenergic Modulation of Cognition. Nature Reviews Neuroscience 2009;10:211–223.

261. Rommelfanger KS, Weinshenker D. Norepinephrine: The Redheaded Stepchild of Parkinson's Disease. Biochemical Pharmacology 2007;74:177–190. [PubMed: 17416354]

262. Biederman J, Spencer T. Attention-Deficit/Hyperactivity Disorder (ADHD) as a Noradrenergic Disorder. Biol. Psychiatry 1999;46:1234–1242. [PubMed: 10560028]

263. Bymaster FP, Katner JS, Nelson DL, et al. Atomoxetine Increases Extracellular Levels of Norepinephrine and Dopamine in Prefrontal Cortex of Rat: A Potential Mechanism for Efficacy in Attention Deficit/Hyperactivity Disorder. Neuropsychopharmacology 2002;27:699–711. [PubMed: 12431845]

264. Southwick SM, Bremner DJ, Rasmusson A, et al. Role of Norepinephrine in the Pathophysiology and Treatment of Posttraumatic Stress Disorder. Biol. Psychiatry 1999;46:1192–1204. [PubMed: 10560025]

265. Ressler KJ, Nemeroff CB. Role of Norepinephrine in the Pathophysiology and Treatment of Mood Disorders. Biol. Psychiatry 1999;46:1219–1233. [PubMed: 10560027]

266. Van Moffaert M, Dierick M. Noradrenaline (Norepinephrine) and Depression: Role in Aetiology and Therapeutic Implications. CNS Drugs 1999;12:293–305.

267. Zhu M-Y, Klimek V, Dilley GE, et al. Elevated Levels of Tyrosine Hydroxylase in the Locus Coeruleus in Major Depression. Biol. Psychiatry 1999;46:1275–1286. [PubMed: 10560033]

268. Ahern TH, Javors MA, Eagles DA, et al. The Effects of Chronic Norepinephrine Transporter Inactivation on Seizure Susceptibility in Mice. Neuropsychopharmacology 2006;31:730–738. [PubMed: 16052243]

269. Klimek V, Stockmeier C, Overholser J, et al. Reduced Levels of Norepinephrine Transporters in the Locus Coeruleus in Major Depression. J. Neurosci 1997;17:8451–8458. [PubMed: 9334417]

270. Logan J, Ding Y-S, Lin K-S, et al. Modeling and Analysis of PET Studies with Norepinephrine Transporter Ligands: The Search for a Reference Region. Nucl. Med. Biol 2005;32:531–542. [PubMed: 15982584]

271. Ding Y-S, Lin K-S, Logan J. PET Imaging of Norepinephrine Transporters. Curr. Pharm. Design 2006;12:3831–3845.

272. Schou M, Pike VW, Halldin C. Development of Radioligands for Imaging of Brain Norepinephrine Transporters *In Vivo* with Positron Emission Tomography. Curr. Topics. Med. Chem 2007;7:1806–1816.

273. Patient Selection and Antidepressant Therapy With Reboxetine, A New Selective Norepinephrine Reuptake Inhibitor. J. Clin. Psychiatry 1998;59

274. Brenner E, Baldwin RM, Tamagnan G. Asymmetric Synthesis of (+)-(*S*,*S*)-Reboxetine via a New (*S*)-2-(Hydroxymethyl)morpholine Preparation. Org. Lett 2005;7:937–939. [PubMed: 15727479]

275. Ding Y-S, Lin K-S, Garza V, et al. Evaluation of a New Norepinephrine Transporter PET Ligand in Baboons, Both in Brain and Peripheral Organs. Synapse 2003;50:345–352. [PubMed: 14556239]

276. Wilson AA, Johnson DP, Mozley D, et al. Synthesis and In Vivo Evaluation of Novel Radiotracers for the In Vivo Imaging of the Norepinephrine Transporter. Nucl. Med. Biol 2003;30:85–92. [PubMed: 12623106]

277. Schou M, Halldin C, Sóvágó J, et al. Specific In Vivo Binding to the Norepinephrine Transporter Demonstrated with the PET Radioligand, (*S*,*S*)-[^{11}C]MeNER. Nucl. Med. Biol 2003;30:707–714. [PubMed: 14499328]

278. Schou M, Halldin C, Sóvágó J, et al. PET Evaluation of Novel Radiofluorinated Reboxetine Analogs as Norepinephrine Transporter Probes in the Monkey Brain. Synapse 2004;53:57–67. [PubMed: 15170818]

279. Schou M, Halldin C, Pike VW, et al. Post-Mortem Human Brain Autoradiography of the Norepinephrine Transporter Using (*S*,*S*)-[^{18}F]FMeNER-D$_2$. Eur. Neuropsychopharmacol 2005;15:517–520. [PubMed: 16139169]

280. Seneca N, Andree B, Sjöholm N, et al. Whole-Body Biodistribution, Radiation Dosimetry Estimates for the PET Norepinephrine Transporter Probe (*S*,*S*)-[^{18}F]FMeNER-D_2 in Non-Human Primates. Nucl. Med. Commun 2005;26:695–700. [PubMed: 16000987]

281. Takano A, Halldin C, Varrone A, et al. Biodistribution and Radiation Dosimetry of the Norepinephrine Transporter Radioligand (*S*,*S*)-[^{18}F]FMeNER-D_2: A Human Whole-Body PET Study. Eur. J. Nucl. Med. Mol. Imaging 2008;35:630–636. [PubMed: 18000665]

282. Seneca N, Gulyás B, Varrone A, et al. Atomoxetine Occupies the Norepinephrine Transporter in a Dose-Dependent Fashion: A PET Study in Nonhuman Primate Brain Using (*S*,*S*)-[^{18}F]FMeNER-D_2. Psychopharmacology 2006;188:119–127. [PubMed: 16896954]

283. Takano A, Gulyás B, Varrone A, et al. Imaging the Norepinephrine Transporter with Positron Emission Tomography: Initial Human Studies with (*S*,*S*)-[^{18}F]FMeNER-D_2. Eur. J. Nucl. Med. Mol. Imaging 2008;35:153–157. [PubMed: 17909794]

284. Lin K-S, Ding Y-S, Kim S-W, et al. Synthesis, Enantiomeric Resolution, F-18 Labeling and Biodistribution of Reboxetine Analogs: Promising Radioligands for Imaging the Norepinephrine Transporter with Positron Emission Tomography. Nucl. Med. Biol 2005;32:415–422. [PubMed: 15878511]

285. Ding Y-S, Lin K-S, Logan J, et al. Comparative Evaluation of Positron Emission Tomography Radiotracers for Imaging the Norepinephrine Transporter: (*S*,*S*) and (*R*,*R*) Enantiomers of Reboxetine Analogs ([^{11}C]Methylreboxetine, 3-Cl-[^{11}C]Methylreboxetine and [^{18}F] Fluororeboxetine), (*R*)-[^{11}C]Nisoxetine, [^{11}C]Oxaprotiline and [^{11}C]Lortalamine. J. Neurochem 2005;94:337–351. [PubMed: 15998285]

286. Zeng F, Jarkas N, Stehouwer JS, et al. Synthesis, In Vitro Characterization, and Radiolabeling of Reboxetine Analogs as Potential PET Radioligands for Imaging the Norepinephrine Transporter. Bioorg. Med. Chem 2008;16:783–793. [PubMed: 17983754]

287. Zeng F, Mun J, Jarkas N, et al. Synthesis Radiosynthesis, and Biological Evaluation of Carbon-11 and Fluorine-18 Labeled Reboxetine Analogues: Potential Positron Emission Tomography Radioligands for in Vivo Imaging of the Norepinephrine Transporter. J. Med. Chem 2009;52:62–73. [PubMed: 19067522]

288. Hara K, Yanagihara N, Minami K, et al. Ketamine Interacts with the Noradrenaline Transporter at a Site Partly Overlapping the Desipramine Binding Site. Naunyn-Schmiedeberg's Arch. Pharmacol 1998;358:328–333.

289. Blough BE, Holmquist CR, Abraham P, et al. 3α-(4-Substituted Phenyl)nortropane-2β-carboxylic Acid Methyl Esters Show Selective Binding at the Norepinephrine Transporter. Bioorg. & Med. Chem. Lett 2000;10:2445–2447. [PubMed: 11078197]

290. Hoepping A, Johnson KM, George C, et al. Novel Conformationally Constrained Tropane Analogues by 6-*endo*-*trig* Radical Cyclization and Stille Coupling - Switch of Activity toward the Serotonin and/or Norepinephrine Transporter. J. Med. Chem 2000;43:2064–2071. [PubMed: 10821718]

291. Tamiz AP, Smith MP, Kozikowski AP. Design, Synthesis and Biological Evaluation of 7-Azatricyclodecanes: Analogues of Cocaine. Bioorg. & Med. Chem. Lett 2000;10:297–300. [PubMed: 10698458]

292. Zhou J, Zhang A, Kläss T, et al. Biaryl Analogues of Conformationally Constrained Tricyclic Tropanes as Potent and Selective Norepinephrine Reuptake Inhibitors: Synthesis and Evaluation of Their Uptake Inhibition at Monoamine Transporter Sites. J. Med. Chem 2003;46:1997–2007. [PubMed: 12723962]

293. Carroll FI, Tyagi S, Blough BE, et al. Synthesis and Monoamine Transporter Binding Properties of 3α-(Substituted phenyl)nortropane-2β-carboxylic Acid Methyl Esters. Norepinephrine Transporter Selective Compounds. J. Med. Chem 2005;48:3852–3857. [PubMed: 15916437]

294. Zhou J, Kläβ T, Johnson KM, et al. Discovery of Novel Conformationally Constrained Tropane-Based Biaryl and Arylacetylene Ligands as Potent and Selective Norepinephrine Transporter Inhibitors and Potential Antidepressants. Bioorg. Med. Chem. Lett 2005;15:2461–2465. [PubMed: 15863297]

295. Zeng F, Jarkas N, Owens MJ, et al. Synthesis and Monoamine Transporter Affinity of Front Bridged Tricyclic 3β-(4′-halo or 4′-methyl)phenyltropanes Bearing Methylene or Carbomethoxymethylene on the Bridge to the 2β-Position. Bioorg. Med. Chem. Lett 2006;16:4661–4663. [PubMed: 16784855]

296. Eildal JNN, Andersen J, Kristensen AS, et al. From the Selective Serotonin Transporter Inhibitor Citalopram to the Selective Norepinephrine Transporter Inhibitor Talopram: Synthesis and Structure-Activity Relationship Studies. J. Med. Chem 2008;51:3045–3048. [PubMed: 18429609]

297. McConathy J, Owens MJ, Kilts CD, et al. Synthesis and Biological Evaluation of [^{11}C]Talopram and [^{11}C]Talsupram: Candidate PET Ligands for the Norepinephrine Transporter. Nucl. Med. Biol 2004;31:705–718. [PubMed: 15246361]

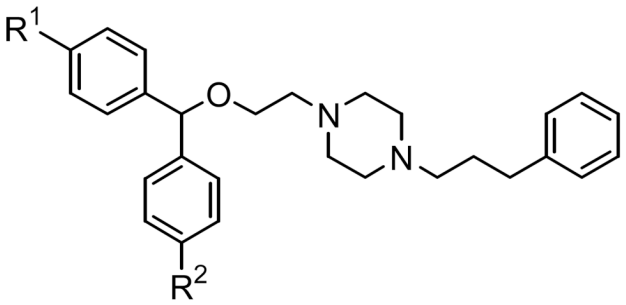

[^{18}F]**1** R^1 = F, R^2 = ^{18}F (GBR 12909)
[^{18}F]**2** R^1 = H, R^2 = ^{18}F (GBR 13119)

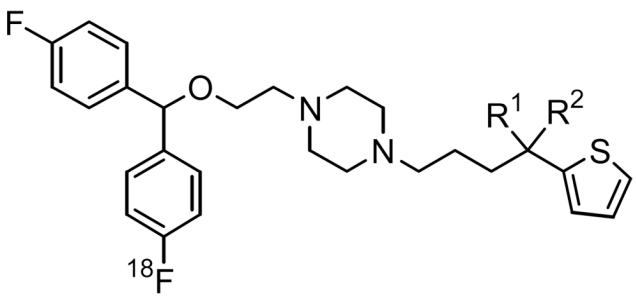

[^{18}F]**3** R^1,R^2 = O (NNC 12-0817)
[^{18}F]**4** R^1 = H, R^2 = OH (NNC 12-0818)

Figure 1.
Structures of GBR-based DAT PET tracers.

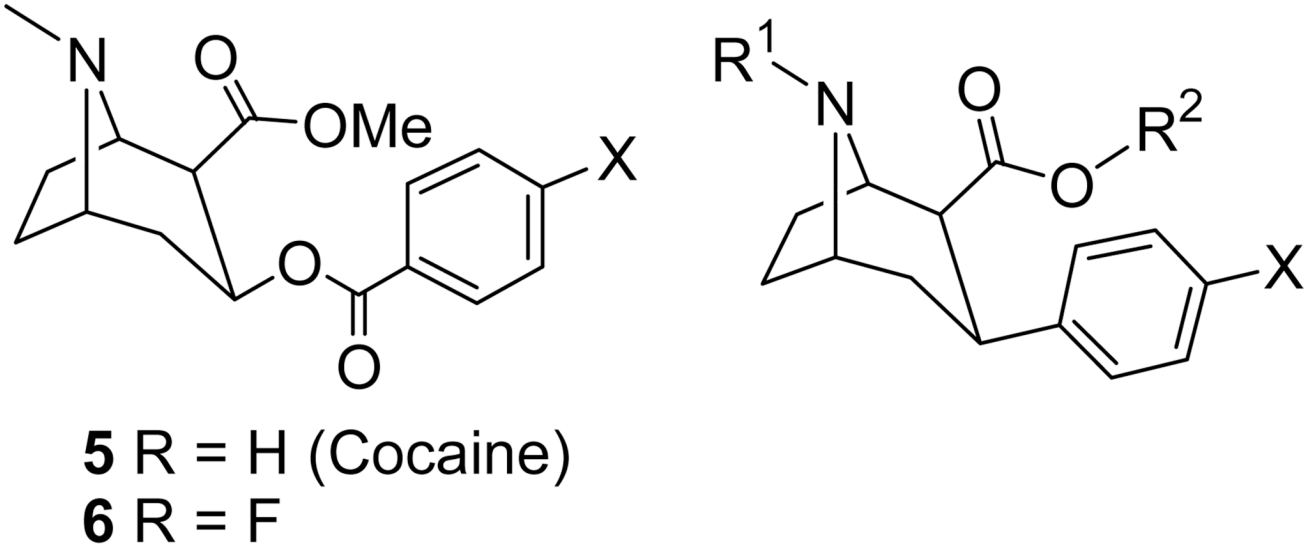

5 R = H (Cocaine)
6 R = F

Fig 2.
Cocaine, 4′-Fluorococaine, and 3β-Phenyl Tropane-Based Dopamine Transporter Ligands.

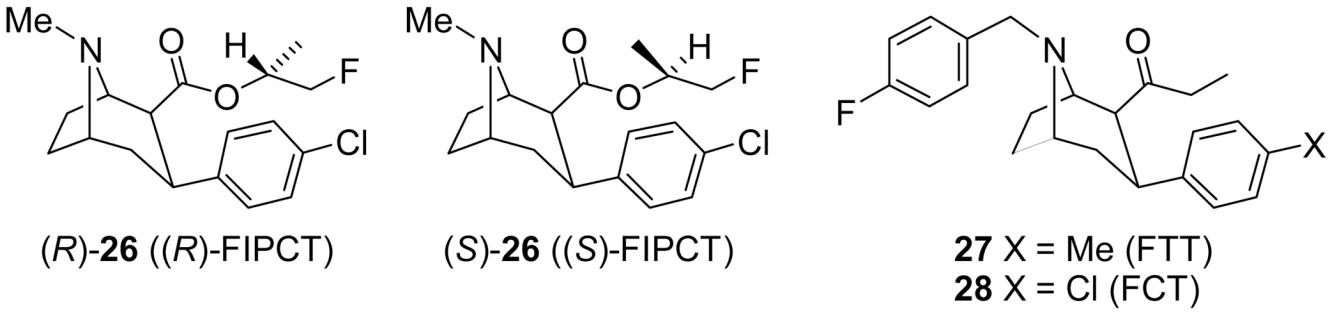

Figure 3.
3β-Phenyl Tropane-Based Dopamine Transporter Ligands.

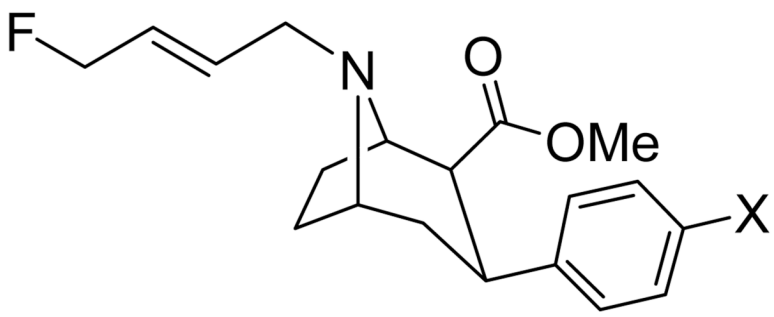

29 X = F (FBFNT)
30 X =Cl (FBClNT)
31 X = Br (FBBrNT)
32 X = I (FBINT)
33 X = Me (LBT-999)

Fig 4.
Binding Affinities of **29**–**32** At Transfected Human Monoamine Transporters.

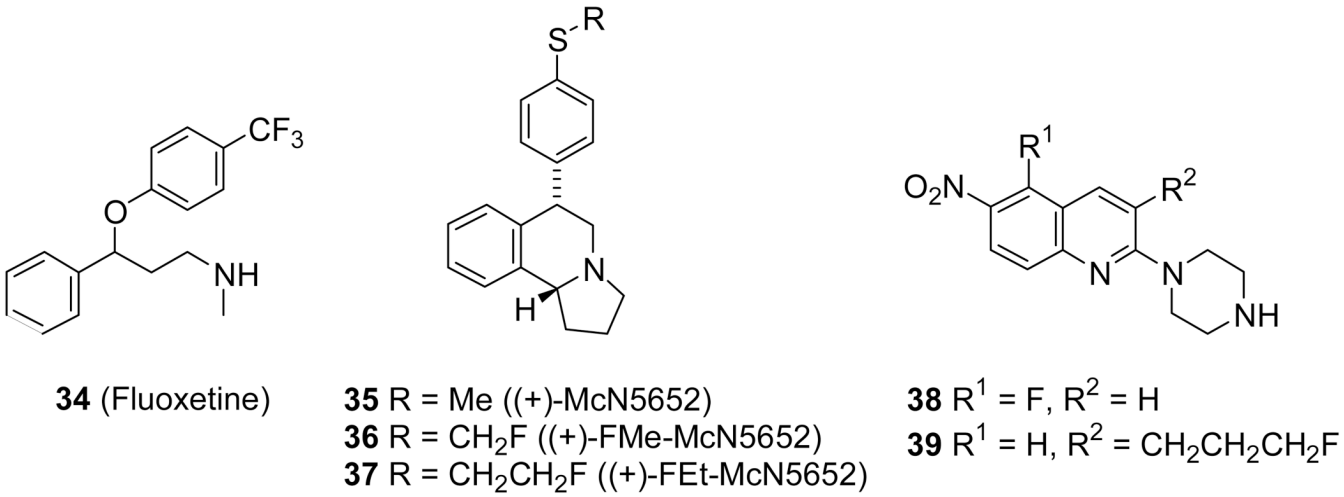

34 (Fluoxetine)

35 R = Me ((+)-McN5652)
36 R = CH_2F ((+)-FMe-McN5652)
37 R = CH_2CH_2F ((+)-FEt-McN5652)

38 R^1 = F, R^2 = H
39 R^1 = H, R^2 = $CH_2CH_2CH_2F$

Figure 5.
SERT Ligands.

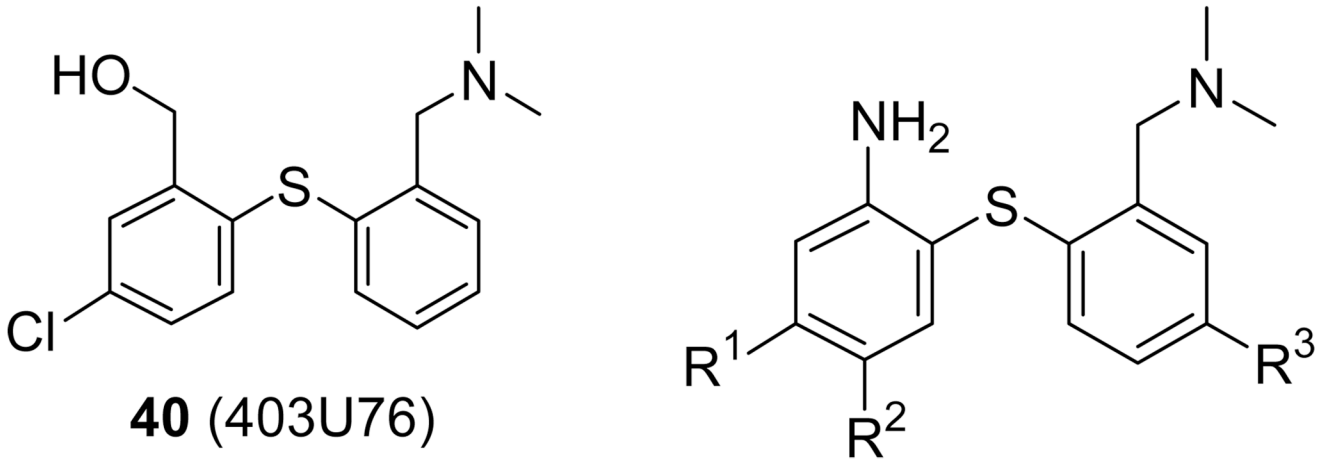

Fig 6.
Diaryl Sulfide-Based Serotonin Transporter Ligands.

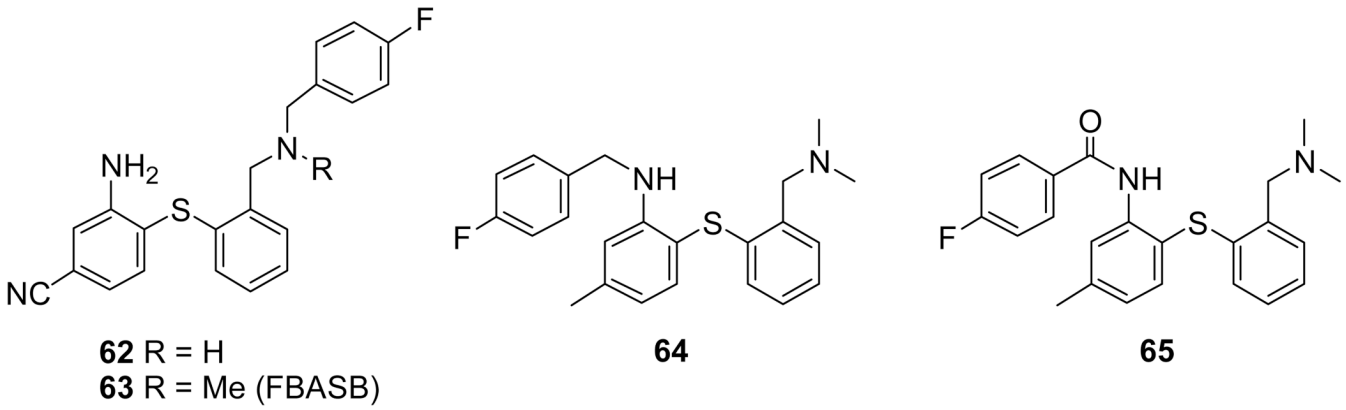

Figure 7.
Diaryl Sulfide-Based Serotonin Transporter Ligands.

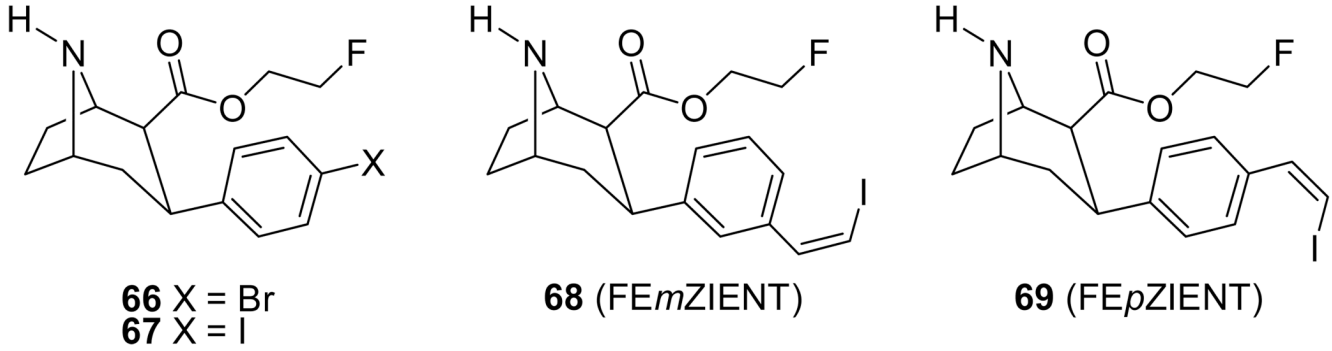

66 X = Br
67 X = I

68 (FE*m*ZIENT)

69 (FE*p*ZIENT)

Figure 8.
Fluoroethyl Ester Nortropane-based SERT Ligands.

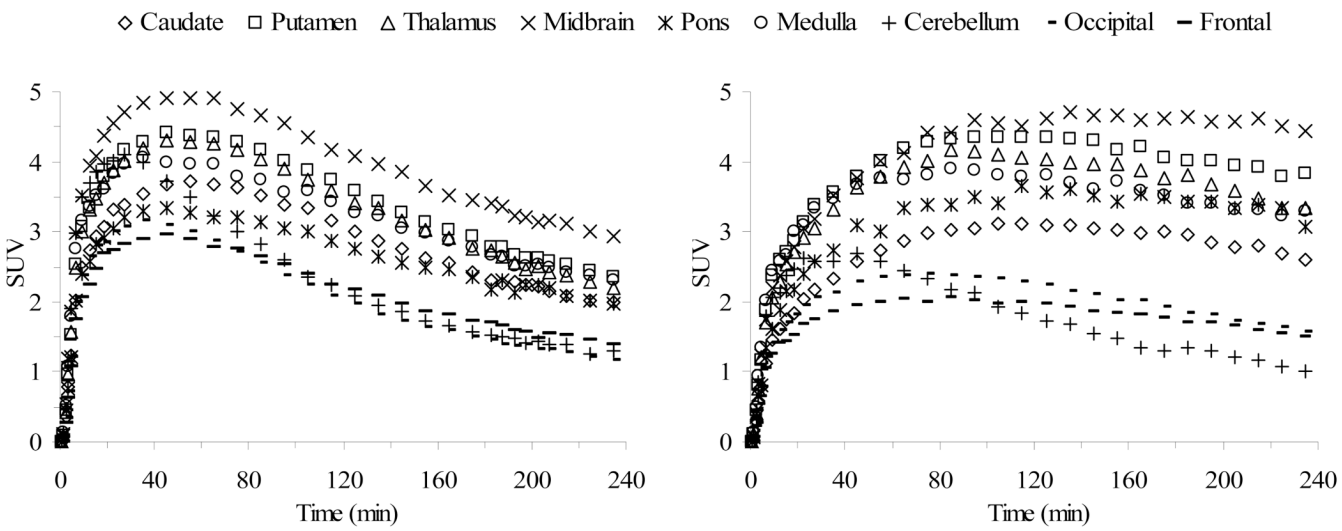

Figure 9.
MicroPET time-activity curves obtained by injection of [^{18}F]**68** (left) and [^{18}F]**69** (right) into anesthetized cynomolgus monkeys.

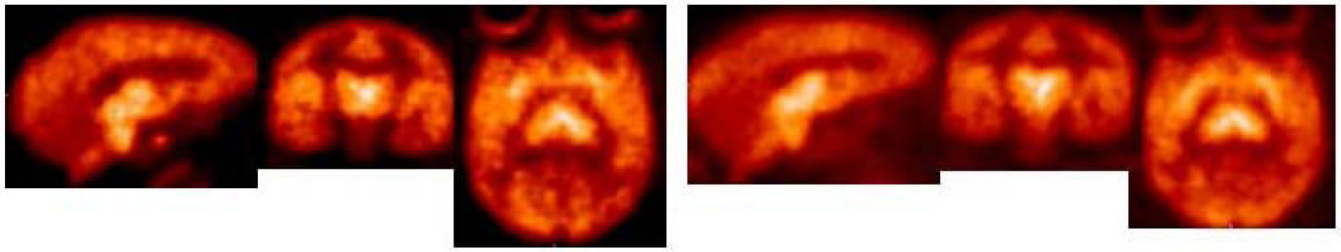

Figure 10.
HRRT PET images obtained by injection of [^{18}F]**68** (left) and [^{18}F]**69** (right) into an awake rhesus monkey.

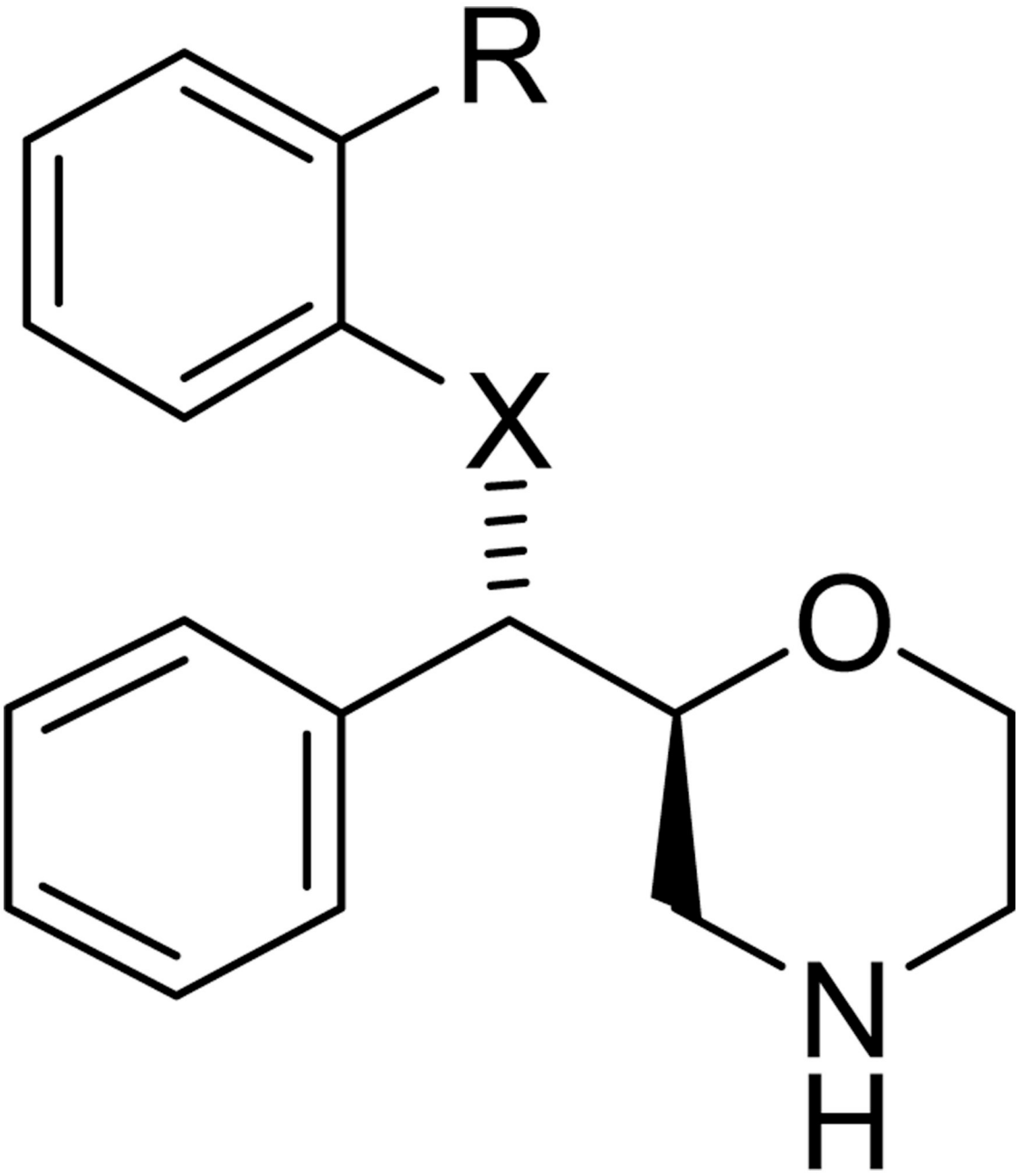

Fig 11.
(*S*,*S*)-Reboxetine Derivative-Based Norepinephrine Transporter Ligands.

Table 1

	Compound	R^1 =	R^2 =	X =
7	WIN 35,065-2	Me	Me	H
8	WIN 35,428; β-CFT	Me	Me	F
9	RTI-31	Me	Me	Cl
10	RTI-51; CBT	Me	Me	Br
11	RTI-55; β-CIT	Me	Me	I
12	RTI-32	Me	Me	Me
13	β-CFT-FE	CH_2CH_2F	Me	F
14	β-CFT-FP	$CH_2CH_2CH_2F$	Me	F
15	FE-β-CIT; β-CIT-FE	CH_2CH_2F	Me	I
16	FP-β-CIT; β-CIT-FP	$CH_2CH_2CH_2F$	Me	I
17		$CH_2CH_2CH_2F$	*i*-Pr	I
18	FECNT	CH_2CH_2F	Me	Cl
19	FPCT	$CH_2CH_2CH_2F$	Me	Cl
20	FPCMT	$CH_2CH_2CH_2F$	Me	Me
21	FPCBT	$CH_2CH_2CH_2F$	Me	Br
22	FETT	Me	CH_2CH_2F	Me
23	FECT	Me	CH_2CH_2F	Cl
24	MCL322	Me	CH_2CH_2F	Br
25	MCL301; FE@CIT	Me	CH_2CH_2F	I

Table 2

Compound	K_i (nM)			Selectivity	
	DAT	SERT	NET	SERT/DAT	NET/DAT
29	1.70	85.5	>10,000	50.3	>5882
30	2.54	24.2	>10,000	9.5	>3937
31	0.24	0.85	91	3.5	379
32	0.17	0.21	57	1.2	335

Table 3

	Compound	R^1	R^2	R^3	K_i (nM) SERT	DAT	NET	Ref.
41	ADAM	I	H	H	0.013	840	699	[209]
42	DASB	CN	H	H	1.10	1423	1350	[211]
43	DAPP	OMe	H	H	1.89	2651	1992	[211]
44	DAPA	Br	H	H	0.38	N/A	N/A	[213]
45	HOMADAM	CH_2OH	H	H	0.57	>1000	144	[218]
46	EADAM	Et	H	H	0.17	>1000	367	[217]
47	AFA,	F	H	H	1.46	>10,000	141.7	[215]
	4-F-ADAM	F	H	H	0.08	2267	117	[222]
48		CF_3	H	H	0.33	2038	1205	[211]
49	AFM	CH_2F	H	H	1.04	>10,000	664	[214]
50	AFE	CH_2CH_2F	H	H	1.80	>10,000	946	[216]
51	AFP	$CH_2CH_2CH_2F$	H	H	3.58	>10,000	505	[223]
52	5-F-ADAM	H	F	H	0.47	N/A	N/A	[224]
53	ACF	Cl	F	H	0.05	3020	650	[225]
54		H	H	OCH_2CH_2F	0.25	340	7.5	[226]
55		F	H	OCH_2CH_2F	0.10	>1000	37	[226]
56		Cl	H	OCH_2CH_2F	0.03	847	97	[226]
57		Br	H	OCH_2CH_2F	0.05	>1000	114	[226]
58		H	H	$OCH_2CH_2CH_2F$	1.4	299	12	[226]
59		F	H	$OCH_2CH_2CH_2F$	0.95	>1000	95	[226]
60		Br	H	$OCH_2CH_2CH_2F$	0.15	>1000	>1000	[226]
61		CH_2OH	H	F	1.26	>2000	618	[227]

PET Clin. Author manuscript; available in PMC 2010 March 8.

Table 4

Compound		X =	R =
70	Reboxetine	O	OCH_2CH_3
71	MeNER	O	OCH_3
72	FMeNER	O	OCH_2F
73	FMeNER-D_2	O	OCD_2F
74	FERB	O	OCH_2CH_2F
75	FERB-D_2	O	OCD_2CD_2F
76	MENET	O	CH_3
77	MESNET	S	CH_3
78	FENET	O	CH_2CH_2F
79	FPNET	O	$CH_2CH_2CH_2F$
80		S	OCH_2CH_2F
81		S	$OCH_2CH_2CH_2F$